

PRIMER ON CEREBROVASCULAR DISEASES

SECOND EDITION

Edited by

LOUIS R. CAPLAN

*Department of Neurology
Beth Israel Deaconess Medical Center
Harvard Medical School
Boston, MA, United States*

JOSÉ BILLER

*Department of Neurology
Loyola University Chicago
Stritch School of Medicine
Maywood, IL, United States*

MEGAN C. LEARY

*Department of Neurology
Lehigh Valley Hospital and Health Network
Allentown, PA, United States
and
Morsani College of Medicine
University of South Florida
Tampa, FL, United States*

ENG H. LO

*Departments of Neurology and Radiology
Massachusetts General Hospital
Harvard Medical School
Boston, MA, United States*

AJITH J. THOMAS

*Division of Neurosurgery
Beth Israel Deaconess Medical Center
Harvard Medical School
Boston, MA, United States*

MIDORI YENARI

*Department of Neurology
University of California, San Francisco
San Francisco Veterans Affairs Medical School
San Francisco, CA, United States*

JOHN H. ZHANG

*Departments of Anesthesiology and Neurosurgery
Loma Linda University School of Medicine
Loma Linda, CA, United States*



ACADEMIC PRESS

An imprint of Elsevier
elsevier.com

Academic Press is an imprint of Elsevier
125 London Wall, London EC2Y 5AS, United Kingdom
525 B Street, Suite 1800, San Diego, CA 92101-4495, United States
50 Hampshire Street, 5th Floor, Cambridge, MA 02139, United States
The Boulevard, Langford Lane, Kidlington, Oxford OX5 1GB, United Kingdom

Copyright © 2017 Elsevier Inc. All rights reserved. Except Chapter 123 “Stroke and Infection: Tuberculosis, Brucellosis, Syphilis, Lyme Disease and Listeriosis” which is in the Public domain.

Cover: Cover design by Lauren J. Lo. Images kindly provided by Dr. José Biller, Dr. Thomas P. Davis, Dr. Joe Herndon, Dr. Dong-Eog Kim, Ms. Caroline Sodja (NRC), and Dr. Danica Stanimirovic. Left panel: immunostaining of ZO-1 (red) and DAPI (blue) in cerebral endothelial cell cultures; Middle panel: angiogram of arteriovenous malformation; Right panel: infarct frequency map derived from a database of 400 diffusion-weighted MRI scans from patients with acute middle cerebral artery strokes; Background: IBA-positive (red) peri-vascular microglia and MHCII-positive (green) cerebral endothelium.

No part of this publication may be reproduced or transmitted in any form or by any means, electronic or mechanical, including photocopying, recording, or any information storage and retrieval system, without permission in writing from the publisher. Details on how to seek permission, further information about the Publisher’s permissions policies and our arrangements with organizations such as the Copyright Clearance Center and the Copyright Licensing Agency, can be found at our website: www.elsevier.com/permissions.

This book and the individual contributions contained in it are protected under copyright by the Publisher (other than as may be noted herein).

Notices

Knowledge and best practice in this field are constantly changing. As new research and experience broaden our understanding, changes in research methods, professional practices, or medical treatment may become necessary.

Practitioners and researchers must always rely on their own experience and knowledge in evaluating and using any information, methods, compounds, or experiments described herein. In using such information or methods they should be mindful of their own safety and the safety of others, including parties for whom they have a professional responsibility.

To the fullest extent of the law, neither the Publisher nor the authors, contributors, or editors, assume any liability for any injury and/or damage to persons or property as a matter of products liability, negligence or otherwise, or from any use or operation of any methods, products, instructions, or ideas contained in the material herein.

Library of Congress Cataloging-in-Publication Data

A catalog record for this book is available from the Library of Congress

British Library Cataloging-in-Publication Data

A catalogue record for this book is available from the British Library

ISBN: 978-0-12-803058-5

For information on all Academic Press publications visit our website at <https://www.elsevier.com/books-and-journals>



Publisher: Mara Conner
Acquisition Editor: Melanie Tucker
Editorial Project Manager: Kristi Anderson
Production Project Manager: Julia Haynes
Designer: Matt Limbert

Typeset by TNQ Books and Journals

List of Contributors

- J.A. Abbatemarco** Lehigh Valley Hospital and Health Network, Allentown, PA, United States
- R.J. Adams** Medical University of South Carolina, Charleston, SC, United States
- D.L. Adkins** Medical University of South Carolina, Charleston, SC, United States
- Y. Akamatsu** University of California, San Francisco and the San Francisco Veterans Affairs Medical Center, San Francisco, CA, United States; Tohoku University Graduate School of Medicine, Sendai, Japan
- O. Akyol** Loma Linda University School of Medicine, Loma Linda, CA, United States
- A.V. Alexandrov** The University of Tennessee Health Science Center, Memphis, TN, United States
- I. Alim** Burke Medical Research Institute, White Plains, NY, United States; Weill Medical College of Cornell University, New York, NY, United States
- A.M. Alkhachroum** University Hospitals Case Medical Center, Neurological Institute, Cleveland, OH, United States
- S. Amin-Hanjani** University of Illinois at Chicago, Chicago, IL, United States
- A.V. Andjelkovic** University of Michigan, Ann Arbor, MI, United States
- J. Anrather** Weill Cornell Medical College, New York, NY, United States
- R. Applegate II** Loma Linda University School of Medicine, Loma Linda, CA, United States
- K. Arai** Harvard Medical School, Boston, MA, United States
- C. Ayata** Harvard Medical School, Boston, MA, United States
- M.A. Aziz-Sultan** Brigham and Women's Hospital, Harvard Medical School, Boston, MA, United States
- I. Ballesteros** Universidad Complutense, Madrid, Spain; Memorial Sloan-Kettering Cancer Center, New York, NY, United States
- B. Bar** Loyola University Chicago, Stritch School of Medicine, Maywood, IL, United States
- F.C. Barone** SUNY Downstate Medical Center, New York, NY, United States
- D.L. Barrow** Emory University School of Medicine, Atlanta, GA, United States
- M.K. Başkaya** University of Wisconsin–Madison, Madison, WI, United States
- K. Bateman** University of Cape Town, Cape Town, South Africa
- N.G. Bazan** Louisiana State University Health New Orleans, New Orleans, LA, United States
- J.S. Beecher** UT Southwestern Medical Center, Dallas, TX, United States
- A. Beer-Furlan** Wexner Medical Center, The Ohio State University, Columbus, OH, United States
- L. Belayev** Louisiana State University Health New Orleans, New Orleans, LA, United States
- P. Bhattacharya** Saint Joseph Mercy Oakland, Pontiac, MI, United States
- R. Bhole** University of Tennessee Health Science Center, Memphis, TN, United States
- J. Biller** Loyola University Chicago, Stritch School of Medicine, Maywood, IL, United States
- V. Biousse** Emory University School of Medicine, Atlanta, GA, United States
- C.V. Borlongan** University of South Florida Morsani College of Medicine, Tampa, FL, United States
- M.J.R.J. Bouts** University Medical Center Utrecht, Utrecht, The Netherlands; Massachusetts General Hospital, Charlestown, MA, United States; Leiden University, Leiden, The Netherlands; Leiden University Medical Center, Leiden, The Netherlands
- R.L. Brey** University of Texas Health Science Center at San Antonio, San Antonio, TX, United States
- R. Bronstein** Stony Brook University, Stony Brook, NY, United States
- A. Bryer** University of Cape Town, Cape Town, South Africa
- K.R. Bulsara** Yale University School of Medicine/Yale New Haven Hospital, New Haven, CT, United States
- A. Can** Harvard Medical School, Boston, MA, United States
- P. Canhão** University of Lisbon, Lisbon, Portugal
- L.R. Caplan** Harvard University, Beth Israel Deaconess Medical Center, Boston, MA, United States
- S.T. Carmichael** University of California Los Angeles, Los Angeles, CA, United States
- R. Carrau** Wexner Medical Center, The Ohio State University, Columbus, OH, United States
- J. Castaldo** Lehigh Valley Hospital and Health Network, Allentown, PA, United States
- L. Catanese** Harvard University, Beth Israel Deaconess Medical Center, Boston, MA, United States
- H. Chabriot** Centre de référence pour les maladies rares des vaisseaux du cerveau et de l'œil (CERVCO), DHU-NeuroVasc and INSERM U1161, Université Denis Diderot, Paris, France

- S. Chaturvedi** University of Miami Miller School of Medicine, Miami, FL, United States
- N. Chaudhary** University of Michigan, Ann Arbor, MI, United States
- Jieli Chen** Henry Ford Hospital, Detroit, MI, United States
- S. Chen** Zhejiang University, Hangzhou, Zhejiang, China
- Jun Chen** University of Pittsburgh, Pittsburgh, PA, United States; Fudan University, Shanghai, China
- D.W. Choi** State University of New York at Stony Brook, Stony Brook, NY, United States; Korea Institute of Science and Technology, Seoul, South Korea
- B. Choi** Massachusetts General Hospital and Harvard Medical School, Boston, MA, United States
- M. Chopp** Henry Ford Hospital, Detroit, MI, United States; Oakland University, Rochester, MI, United States
- D.Y. Chung** Harvard Medical School, Boston, MA, United States
- C.-P. Chung** Taipei Veterans General Hospital, National Yang Ming University, Taipei, Taiwan
- M.J. Cipolla** University of Vermont, Burlington, VT, United States
- F. Colbourne** University of Alberta, Edmonton, AB, Canada
- Q. Colburn** University of South Florida Morsani College of Medicine, Tampa, FL, United States
- B.J. Cord** Yale University School of Medicine/Yale New Haven Hospital, New Haven, CT, United States
- B.M. Coull** The University of Arizona College of Medicine, Tucson, AZ, United States
- M.I. Cuartero** Universidad Complutense, Madrid, Spain; Instituto de Investigación Hospital 12 de Octubre (i+12), Madrid, Spain
- J.L. Cummings** Cleveland Clinic Las Vegas, NV, United States; Cleveland Clinic Lerner College of Medicine of Case Western Reserve University, Cleveland, OH, United States
- R.M. Dafer** Rush University Medical Center, Chicago, IL, United States
- T. Dalkara** Hacettepe University, Ankara, Turkey
- B. Daou** Thomas Jefferson University and Jefferson Hospital for Neuroscience, Philadelphia, PA, United States
- K.R. Dave** University of Miami, Miami, Florida, United States
- T.P. Davis** University of Arizona, Tucson, AZ, United States
- M. De Georgia** University Hospitals Case Medical Center, Neurological Institute, Cleveland, OH, United States
- T.M. De Silva** The University of Iowa Carver College of Medicine, Iowa City, IA, United States; Monash University, Clayton, VIC, Australia
- A. Dharap** JFK Medical Center, Edison, NJ, United States
- M.R. Di Tullio** Columbia University, New York, NY, United States
- W.D. Dietrich** University of Miami Miller School of Medicine, Miami, FL, United States
- R.M. Dijkhuizen** University Medical Center Utrecht, Utrecht, The Netherlands
- B.H. Dobkin** University of California Los Angeles, Los Angeles, CA, United States
- R. Du** Harvard Medical School, Boston, MA, United States
- A.F. Ducruet** University of Pittsburgh, Pittsburgh, PA, United States
- K.R. Duncan** Lehigh Valley Hospital and Health Network, Allentown, PA, United States
- L. Edvinsson** Lund University Hospital, Lund, Sweden
- M.J. Edwards** St Georges University of London, London, United Kingdom
- E. Egemen** Koç University Hospital, Istanbul, Turkey
- M. El-Hunjul** Lehigh Valley Hospital and Health Network, Allentown, PA, United States
- M. Emanuele** Loyola University Chicago, Stritch School of Medicine, Maywood, IL, United States
- N. Emanuele** Hines VA Medical Center, Hines, IL, United States
- M.K. Erdman** Los Angeles County Hospital and USC Medical Center, Los Angeles, CA, United States
- A. Ergul** Augusta University, Augusta, GA, United States
- S.C. Fagan** University of Georgia College of Pharmacy, Augusta, GA, United States
- F.M. Faraci** The University of Iowa Carver College of Medicine, Iowa City, IA, United States
- C. Federau** Stanford University, Stanford, CA, United States
- J.M. Ferro** University of Lisbon, Lisbon, Portugal
- M. Fisher** University of California, Irvine, Irvine, CA, United States
- K.D. Flemming** Mayo Clinic, Rochester, MN, United States
- C. Foerch** Goethe University, Frankfurt am Main, Germany
- R.S. Freitas** Louisiana State University Health New Orleans, New Orleans, LA, United States
- R.M. Friedlander** University of Pittsburgh, Pittsburgh, PA, United States
- T. Gaberel** Harvard Medical School, Boston, MA, United States
- C. Gakuba** Harvard Medical School, Boston, MA, United States
- R.G. Giffard** Stanford University School of Medicine, Stanford, CA, United States
- M.P. Goldberg** UT Southwestern Medical Center, Dallas, TX, United States
- R.G. González** Harvard Medical School, Boston, MA, United States
- S. Gopinath** Baylor College of Medicine, Houston, TX, United States
- P.B. Gorelick** Mercy Health Hauenstein Neurosciences, Grand Rapids, MI, United States; Michigan State University College of Human Medicine, East Lansing, MI, United States

- C. Goshgarian** Mercy Health Hauenstein Neurosciences, Grand Rapids, MI, United States
- D.A. Greenberg** Buck Institute for Research on Aging, Novato, CA, United States
- C.J. Griessenauer** Harvard Medical School, Boston MA, United States
- K.A. Groshans** Walter Reed National Military Medical Center, Bethesda, MD, United States
- R. Gupta** Wellstar Health System, Marietta, GA, United States
- R.A. Hachem** Wexner Medical Center, The Ohio State University, Columbus, OH, United States
- Z.A. Hage** University of Illinois at Chicago, Chicago, IL, United States
- E.D. Hall** University of Kentucky College of Medicine, Lexington, KY, United States
- E. Hamel** McGill University, Montréal, QC, Canada
- Q. Hao** The Johns Hopkins University School of Medicine, Baltimore, MD, United States
- A.S. Haqqani** National Research Council of Canada, Ottawa, ON, Canada
- R. Hariman** Medical College of Wisconsin, Milwaukee, WI, United States
- D. Hasan** University of Iowa Hospital and Clinics, Iowa City, IA, United States
- D.C. Haussen** Emory University School of Medicine, Atlanta, GA, United States
- L. He** Vanderbilt University, Nashville, TN, United States
- D.M. Heiferman** Loyola University Chicago, Stritch School of Medicine, Maywood, IL, United States
- J.M. Herndon** University of Arizona, Tucson, AZ, United States
- W.M. Ho** Loma Linda University School of Medicine, Loma Linda, CA, United States
- S. Hoffmann** Charité – Universitätsmedizin Berlin, Berlin, Germany
- B.M. Howard** Emory University School of Medicine, Atlanta, GA, United States
- B.R. Hu** Shock Trauma and Anesthesiology Research Center, University of Maryland School of Medicine, Baltimore, MD, United States
- J.D. Huber** West Virginia University, Morgantown, WV, United States
- B. Huisa** University of California San Diego, San Diego, CA, United States
- P.D. Hurn** University of Michigan, School of Nursing, Ann Arbor, MI, United States
- J.J. Iliff** Oregon Health & Science University, Portland, OR, United States; University of Rochester Medical Center, Rochester, NY, United States
- P. Jabbour** Thomas Jefferson University and Jefferson Hospital for Neuroscience, Philadelphia, PA, United States
- A.O. Jamshidi** Wexner Medical Center, The Ohio State University, Columbus, OH, United States
- B. Jankowitz** University of Pittsburgh Medical Center, Pittsburgh, PA, United States
- G.C. Jickling** University of California at Davis, Sacramento, CA, United States
- M. Johansen** The Johns Hopkins University School of Medicine, Baltimore, MD, United States
- T.G. Jovin** University of Pittsburgh Medical Center, Pittsburgh, PA, United States
- S.S. Karuppagounder** Burke Medical Research Institute, White Plains, NY, United States; Weill Medical College of Cornell University, New York, NY, United States
- E.M. Kasper** Harvard Medical School, Boston, MA, United States
- R.F. Keep** University of Michigan, Ann Arbor, MI, United States
- H.-H. Kim** Harvard Medical School, Boston, MA, United States
- D.E. Kim** Dongguk University, Goyang, Republic of Korea
- J.S. Kim** Asan Medical Center, University of Ulsan, Seoul, South Korea
- J.Y. Kim** University of California, San Francisco and the San Francisco Veterans Affairs Medical Center, San Francisco, CA, United States
- A.C. Klahr** University of Alberta, Edmonton, AB, Canada
- M.J. Koch** Massachusetts General Hospital and Harvard Medical School, Boston, MA, United States
- M. Kole** Henry Ford Health System, Detroit, MI, United States
- S.M. Koleilat** The University of Arizona College of Medicine, Tucson, AZ, United States
- A. Kozaan** University of Wisconsin–Madison, Madison, WI, United States
- S. Kuroda** University of Toyama, Toyama, Japan; Hokkaido University Graduate School of Medicine, Sapporo, Japan
- C. Lamy** Paris Descartes University, Paris, France
- G. Lanzino** Mayo Clinic, Rochester, MN, United States
- A.G. Larsen** Harvard Medical School, Boston, MA, United States
- Y. Laviv** Harvard Medical School, Boston, MA, United States
- M.T. Lawton** University of California, San Francisco, San Francisco, CA, United States
- M.C. Leary** Lehigh Valley Hospital and Health Network, Allentown, PA, United States; University of South Florida, Tampa, FL, United States
- E.C. Leira** University of Iowa, Iowa City, IA, United States
- L. Li** Stanford University School of Medicine, Stanford, CA, United States
- Q. Li** The Johns Hopkins University School of Medicine, Baltimore, MD, United States

- D.S. Liebeskind** University of California, Los Angeles, Los Angeles, CA, United States
- L. Lin** Harvard Medical School, Boston, MA, United States; Wenzhou Medical University Wenzhou, People's Republic of China
- V.A. Lioutas** Beth Israel Deaconess Medical Center, Boston, MA, United States
- T. Lippert** University of South Florida Morsani College of Medicine, Tampa, FL, United States
- R. Liu** University of North Texas Health Science Center, Fort Worth, TX, United States
- J. Liu** University of California, San Francisco and the San Francisco Veterans Affairs Medical Center, San Francisco, CA, United States
- C.L. Liu** Shock Trauma and Anesthesiology Research Center, University of Maryland School of Medicine, Baltimore, MD, United States
- I. Lizasoain** Universidad Complutense, Madrid, Spain; Instituto de Investigación Hospital 12 de Octubre (i+12), Madrid, Spain
- E.H. Lo** Harvard Medical School, Boston, MA, United States
- C.M. Loftus** Loyola University Chicago, Stritch School of Medicine, Maywood, IL, United States
- A.F. Logsdon** West Virginia University, Morgantown, WV, United States
- B.P. Lucke-Wold** West Virginia University, Morgantown, WV, United States
- S. Madhavan** University of Illinois Chicago, Chicago, IL, United States
- V. Madhugiri** Stanford University School of Medicine, Stanford, CA, United States
- K. Malhotra** University of California, Los Angeles, Los Angeles, CA, United States
- W.J. Manning** Harvard Medical School, Boston, MA, United States
- S.J. Marcell** Louisiana State University Health New Orleans, New Orleans, LA, United States
- J.-L. Mas** Paris Descartes University, Paris, France
- K. Masamoto** University of Electro-Communications, Chofu, Tokyo, Japan
- C. Matute** Achucarro Basque Center for Neuroscience, Zamudio, Spain; CIBERNED, Madrid, Spain; Universidad del País Vasco-UPV/EHU, Leioa, Spain
- L.D. McCullough** The University of Texas Health Science Center at Houston, Houston, TX, United States
- M.M. McDowell** University of Pittsburgh, Pittsburgh, PA, United States
- M. Mehdiratta** Trillium Health Partners, Mississauga, ON, Canada; University of Toronto, Toronto, ON, Canada
- D. Mehta** Lehigh Valley Hospital and Health Network, Allentown, PA, United States
- A. Meisel** Charité – Universitätsmedizin Berlin, Berlin, Germany
- J. Messegee** University of New Mexico, Albuquerque, NM, United States
- B. Miller** University Hospitals Case Medical Center, Neurological Institute, Cleveland, OH, United States
- S. Mirza** UT Southwestern Medical Center, Dallas, TX, United States
- J.M. Modak** Beth Israel Deaconess Medical Center, Boston, MA, United States
- M.A. Moro** Universidad Complutense, Madrid, Spain; Instituto de Investigación Hospital 12 de Octubre (i+12), Madrid, Spain
- M.A. Nagel** University of Colorado School of Medicine, Aurora, CO, United States
- S. Namura** Morehouse School of Medicine, Atlanta, GA, United States
- M. Nedergaard** University of Rochester Medical Center, Rochester, NY, United States; University of Copenhagen, Copenhagen, Denmark
- D.W. Newell** Seattle Neuroscience Institute, Seattle, WA, United States
- N.J. Newman** Emory University School of Medicine, Atlanta, GA, United States
- K.L. Ng** University of California Los Angeles, Los Angeles, CA, United States
- D. Nguyen** University of California San Diego, San Diego, CA, United States
- H. Nguyen** University of South Florida Morsani College of Medicine, Tampa, FL, United States
- G. Nielsen** UCL Institute of Neurology, London, United Kingdom
- Y. Nishijima** University of California, San Francisco and the San Francisco Veterans Affairs Medical Center, San Francisco, CA, United States; Tohoku University Graduate School of Medicine, Sendai, Japan
- N. Nishimura** Cornell University, Ithaca, NY, United States
- R.G. Nogueira** Emory University School of Medicine, Atlanta, GA, United States
- C.S. Ogilvy** Harvard Medical School, Boston, MA, United States
- D.B. Orbach** Boston Children's Hospital/Harvard Medical School, Boston, MA, United States
- A.P. Ostendorf** Ohio State College of Medicine, Columbus, OH, United States
- B. Otto** Wexner Medical Center, The Ohio State University, Columbus, OH, United States
- A. Ozpinar** University of Pittsburgh Medical Center, Pittsburgh, PA, United States
- D.M. Panczykowski** University of Pittsburgh Medical Center, Pittsburgh, PA, United States
- A.B. Patel** Massachusetts General Hospital and Harvard Medical School, Boston, MA, United States
- Y. Perez** Trillium Health Partners, Mississauga, ON, Canada; University of Toronto, Toronto, ON, Canada

- M.A. Perez-Pinzon** University of Miami, Miami, Florida, United States
- C. Potey** University of British Columbia, Vancouver, BC, Canada
- J.M. Pradillo** Universidad Complutense, Madrid, Spain; Instituto de Investigación Hospital 12 de Octubre (i+12), Madrid, Spain
- D.M. Prevedello** Wexner Medical Center, The Ohio State University, Columbus, OH, United States
- K. Rajamani** Wayne State University School of Medicine, Detroit, MI, United States
- L. Rangel-Castilla** University at Buffalo, State University of New York, Buffalo, NY, United States
- N.M. Rao** David Geffen School of Medicine at University of California, Los Angeles, Los Angeles, CA, United States
- R.R. Ratan** Burke Medical Research Institute, White Plains, NY, United States; Weill Medical College of Cornell University, New York, NY, United States
- A.P. Raval** University of Miami, Miami, Florida, United States
- G.D. Reddy** Baylor College of Medicine, Houston, TX, United States
- C. Reis** Loma Linda University Medical Center, Loma Linda, CA, United States
- E.S. Roach** Ohio State College of Medicine, Columbus, OH, United States
- P.T. Ronaldson** University of Arizona, Tucson, AZ, United States
- C.L. Rosen** West Virginia University, Morgantown, WV, United States
- G.A. Rosenberg** The University of New Mexico, Albuquerque, NM, United States
- W.C. Rutledge** University of California, San Francisco, San Francisco, CA, United States
- R. Sabzwari** Loyola University Medical Center and Edward Hines Jr. Veteran Administration Hospital, Hines, IL, United States
- G. Salzano** Northeastern University, Boston, MA, United States
- P.A. Santucci** Loyola University Chicago, Stritch School of Medicine, Maywood, IL, United States
- J.L. Saver** David Geffen School of Medicine at University of California, Los Angeles, Los Angeles, CA, United States
- T. Schallert** The University of Texas at Austin, Austin, TX, United States
- M.L. Schermerhorn** Beth Israel Deaconess Medical Center, Boston, MA, United States
- M.J. Schneck** Loyola University Chicago, Stritch School of Medicine, Maywood, IL, United States
- A.P. See** Brigham and Women's Hospital; Boston Children's Hospital/Harvard Medical School, Boston, MA, United States
- H.J. Shakir** University at Buffalo, State University of New York, Buffalo, NY, United States
- F.R. Sharp** University of California at Davis, Sacramento, CA, United States
- F. Shuja** Beth Israel Deaconess Medical Center, Boston, MA, United States
- A.H. Siddiqui** University at Buffalo, State University of New York, Buffalo, NY, United States
- M.A. Silva** Harvard Medical School, Boston, MA, United States
- A.B. Singhal** Massachusetts General Hospital and Harvard Medical School, Boston, MA, United States
- K. Sivakumar** Lehigh Valley Hospital and Health Network, Allentown, PA, United States
- D.H. Slade** Loyola University Medical Center and Edward Hines Jr. Veteran Administration Hospital, Hines, IL, United States
- E.R. Smith** Harvard Medical School, Boston, MA, United States
- F. Sohrabji** Texas A&M Health Science Center, Bryan, TX, United States
- I. Solaroglu** Koç University, Istanbul, Turkey
- S.K. Sriraman** Northeastern University, Boston, MA, United States
- B. Stamova** University of California at Davis, Sacramento, CA, United States
- D.B. Stanimirovic** National Research Council of Canada, Ottawa, ON, Canada
- C.J. Stapleton** Massachusetts General Hospital and Harvard Medical School, Boston, MA, United States
- C.M. Stary** Stanford University School of Medicine, Stanford, CA, United States
- G.K. Steinberg** Stanford University School of Medicine, Stanford, CA, United States
- C. Stephen** Massachusetts General Hospital, Boston, MA, United States
- R.A. Stetler** University of Pittsburgh, Pittsburgh, PA, United States; Fudan University, Shanghai, China
- J. Stone** University of Edinburgh, Edinburgh, United Kingdom
- R. Sumbria** Keck Graduate Institute, Claremont, CA, United States; University of California, Irvine, Irvine, CA, United States
- R. Sweis** Loyola University Chicago, Stritch School of Medicine, Maywood, IL, United States
- R. Tahir** Henry Ford Health System, Detroit, MI, United States
- R. Tarawneh** Cleveland Clinic, Cleveland, OH, United States; Cleveland Clinic Lerner College of Medicine of Case Western Reserve University, Cleveland, OH, United States
- J. Tarsia** Ochsner Health Systems, New Orleans, LA, United States
- R. Tehrani** Loyola University Chicago, Stritch School of Medicine, Maywood, IL, United States

- M.K. Teo** Stanford University School of Medicine, Stanford, CA, United States
- E.D. Testai** University of Illinois at Chicago, Chicago, IL, United States
- A.S. Thrane** University of Rochester Medical Center, Rochester, NY, United States; Haukeland University Hospital, Bergen, Norway
- M.K. Tobin** University of Illinois at Chicago, Chicago, IL, United States
- M.E. Tome** University of Arizona, Tucson, AZ, United States
- M.A. Topcuoglu** Massachusetts General Hospital and Harvard Medical School, Boston, MA, United States; Hacettepe University Hospitals, Ankara, Turkey
- C.H. Topel** University of Texas Health Science Center at San Antonio, San Antonio, TX, United States
- V. Torchilin** Northeastern University, Boston, MA, United States; King Abdulaziz University, Jeddah, Saudi Arabia
- R.J. Traystman** University of Colorado Denver, Aurora, CO, United States
- S.E. Tsirka** Stony Brook University, Stony Brook, NY, United States
- Y. Turan** University of Wisconsin–Madison, Madison, WI, United States
- M. Tymianski** Krembil Research Institute, Toronto, ON, Canada; University of Toronto, Toronto, ON, Canada; University Health Network, Toronto, ON, Canada
- K. van Leyen** Massachusetts General Hospital, Charlestown, MA, United States; Harvard Medical School, Boston, MA, United States
- P. Varade** Lehigh Valley Hospital and Health Network, Allentown, PA, United States; University of South Florida, Tampa, FL, United States
- J.S. Veluz** St. Mary Medical Center, Langhorne, PA, United States
- R. Vemuganti** University of Wisconsin, Madison, WI, United States
- P. Venkat** Henry Ford Hospital, Detroit, MI, United States; Oakland University, Rochester, MI, United States
- Z.S. Vexler** University of California, San Francisco, San Francisco, CA, United States
- C.M. Vial** Sutter Health/Palo Alto Medical Foundation, Palo Alto, CA, United States
- H.V. Vinters** David Geffen School of Medicine at University of California, Los Angeles, Los Angeles, CA, United States
- M.R. Vosko** Kepler Universitätsklinikum, Linz, Austria
- C. Waeber** University College Cork, Cork, Ireland
- B.P. Walcott** University of California, San Francisco, San Francisco, CA, United States
- J. Wang** The Johns Hopkins University School of Medicine, Baltimore, MD, United States
- X. Wang** Harvard Medical School, Boston, MA, United States
- Y.T. Wang** University of British Columbia, Vancouver, BC, Canada
- Z.Z. Wei** Emory University School of Medicine and Atlanta Veterans Affairs Medical Center, Decatur, GA, United States
- L. Wei** Emory University School of Medicine, Atlanta, GA, United States
- B.G. Welch** UT Southwestern Medical Center, Dallas, TX, United States
- H.R. Winn** Mount Sinai Medical School, New York, NY, United States; University of Iowa, Iowa City, IA, United States
- M. Wintermark** Stanford University, Stanford, CA, United States
- R.J. Wityk** The Johns Hopkins University School of Medicine, Baltimore, MD, United States
- O. Wu** Massachusetts General Hospital, Charlestown, MA, United States
- K.C. Wu** Brigham and Women’s Hospital, Boston, Harvard Medical School, MA, United States
- G. Xi** University of Michigan, Ann Arbor, MI, United States
- H.A. Yacoub** Lehigh Valley Hospital and Health Network, Allentown, PA, United States
- A. Yakhkind** Brown University, Providence, RI, United States
- Y. Yamamoto** Kyoto Katsura Hospital, Kyoto, Japan
- S.-H. Yang** University of North Texas Health Science Center, Fort Worth, TX, United States
- M. Yenari** University of California, San Francisco and the San Francisco Veterans Affairs Medical Center, San Francisco, CA, United States
- K. Yigitkanli** Polatli Government Hospital, Ankara, Turkey
- H. Yonas** University of New Mexico, Albuquerque, NM, United States
- Z. Yu** Harvard Medical School, Boston, MA, United States
- S.L. Zettervall** Beth Israel Deaconess Medical Center, Boston, MA, United States
- J. Zhang** Loma Linda University Medical Center; Loma Linda University School of Medicine, Loma Linda, CA, United States
- W. Zhang** University of Pittsburgh, Pittsburgh, PA, United States; Fudan University, Shanghai, China
- H. Zhao** Stanford University, Stanford, CA, United States

Introduction

Twenty years have passed since the first edition of *Primer on Cerebrovascular Diseases* was published.¹ The book sought to reduce the growing gap in the cerebrovascular field between physicians and surgeons who actively treated patients and researchers who worked in basic and clinical research. The term “translational medicine” was first being discussed at that time. All agreed that the best way to ensure progress was intimate communication and cooperation between clinicians and researchers. Clinicians needed to have some sense about what was happening and forthcoming from the laboratory and researchers needed to know what were the most important targets to help patient care at the bedside and in the clinic. Dr. Arthur Kornberg, who received the Nobel Prize in Physiology and Medicine in 1959 for his work on DNA, commented in his autobiography² that the single most important year in his training was his clinical internship. That exposure provided targets for needed advancement for his entire career, which was spent in various basic research laboratories.

During the past two decades since publication of the first edition, the clinical-research gap has probably widened. Clinicians and surgeons have become even more specialized, each dealing with more restricted situations, technology, compounds, and conditions. Basic researchers have had to become even more competitive for grants. Many work in very specialized areas. I have been at Princeton Cerebrovascular Disease Conference meetings in which all attendees are instructed to sit through all sessions—researchers listening to clinical topics and clinicians taking in research discussions. My sense was that these did not work well. Clinical and research topics were too focused; researchers lacked the clinical

background to place the discussions into perspective and clinicians were at sea in the biochemical and technical details of the basic discussions. A few days was too short a time for the education needed.

This second edition of the *Primer* is aimed directly at providing a clinical-research interface, a repository of information that is basic, concise, simply written, and easily understood for individuals who are unfamiliar with a particular topic. Unlike a short meeting, a volume (hard copy or e-book) can serve as a frequently perused source of information that can bridge a large educational-informational gap. This edition has expanded with more editors and more topics. Editors have carefully selected authors who are working within their topics. They are instructed to make their chapters concise and easily understood. The volume has been thoroughly edited to ensure simplicity and completeness. I hope that it will help reduce the gap and aid progress in translational research and in the clinical care of future stroke patients.

Louis R. Caplan, MD
Boston, Massachusetts
November 2016

1. Caplan LR, Siesjo BK, Weir B, Welch KM, Reis DJ. *Primer on Cerebrovascular Diseases*, San Diego, Academic press, 1997
2. Kornberg A. *For the love of enzymes. The odyssey of a biochemist*. Harvard U press, Cambridge, 1989

Cerebrovascular Anatomy and Hemodynamics

R.J. Traystman

University of Colorado Denver, Aurora, CO, United States

INTRODUCTION

The adult human brain represents about 2% of total body weight, but receives nearly 15% of total resting cardiac output. Under normal conditions, the brain is highly perfused and is extremely sensitive to any change or interruption in its blood supply. If the brain's circulation is completely obstructed, loss of consciousness occurs within seconds and irreversible pathological changes occur within minutes. For example, in cardiac arrest, the extent of injury of the central nervous system (CNS) is the critical factor that determines the degree of recovery. It is, therefore, not surprising that the physiological mechanisms that regulate cerebral circulation are designed to ensure the constancy of cerebral blood flow (CBF) over a broad range of internal and external conditions. This may even occur at the expense of adequate blood flow to other organs.

ANATOMICAL CONSIDERATIONS

Arterial System

The brain of essentially all mammalian species is supplied with blood from several major sources, that is, the internal and external carotid, vertebral, and spinal anterior arteries. However, the relative importance of these channels in any species is unclear. Although the internal carotid artery leads directly to the brain, in some species this vessel is unimportant, and it may be the external carotid that carries the major proportion of blood reaching the brain. In humans, the anterior three-fifths of the cerebrum, except for parts of the occipital and temporal lobes, are supplied by the carotid arteries. The posterior two-fifths of the cerebrum, the cerebellum, and brain stem are supplied by the vertebral-basilar system. The carotid and vertebral arteries unite at the

base of the brain to form the circle of Willis (Fig. 1.1 [1]). This vascular ring then gives rise to three pairs of arteries, the anterior, middle, and posterior cerebral arteries, which cover the external surface of the corresponding regions of the cerebral cortex. These arteries divide into progressively smaller arteries, penetrating brain tissue and supplying blood to specific regions. Branches of the vertebral and basilar arteries form the blood supply for the cerebellum and brain stem. While there is some variability among individuals, the internal carotids and the vertebral-basilar system generally contribute equally to the circle of Willis. Even though the internal carotid and basilar arteries converge (forming the circle of Willis), blood from the two tributaries normally does not mix completely because blood pressure in each arterial tributary is almost equal. Angiography and/or dye injections indicate that blood from the various tributaries is ultimately distributed to relatively specific and delineated brain regions. Under normal conditions, vertebral-basilar arterial blood is mainly distributed to tissues in the posterior fossa while the internal carotids supply the remainder of the brain. In addition, there is relatively little bilateral crossing, again due to the similarity in blood pressure. Normally the circle of Willis functions primarily as an anterior-posterior shunt than as a side-to-side shunt. However, under pathological conditions, especially those that involve focal obstructions in arterial feeders to the circle, the balance of pressures may be altered and the circle of Willis can then serve either as an anterior-posterior or as a side-to-side shunt.

In addition, there are a number of arterial anastomotic vessels on each side of the head between the intracranial and extracranial circulations. These include: (1) a connection between the vertebral and occipital arteries; (2) a communication between the ascending pharyngeal and internal carotid arteries; (3) the middle meningeal artery branching off from the internal maxillary artery and connecting with the internal carotid artery, (4) the anastomotic

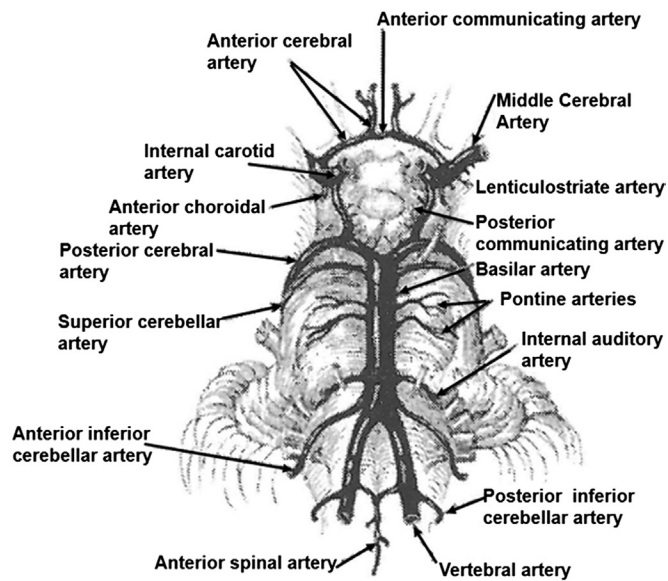


FIGURE 1.1 Major cerebral arteries and the circle of Willis. Modified from Chusid JG. *Correlative neuroanatomy and functional neurology*, 14th ed. Los Altos, CA: Lange Medical Publishers; 1970.

artery between the internal maxillary and internal carotid arteries, (5) pathways between the external and internal ophthalmic arteries, (6) anastomosis between the external and internal ethmoidal arteries, (7) collaterals between the vertebral and the omocervical arteries, and (8) connections between the spinal anterior and vertebral arteries. In some species the external carotid system branches into a complicated network of arteries, the rete mirabile, prior to its entrance to the circle of Willis. This rete system has been proposed to be involved in a heat-exchange counter-current mechanism, which acts to lower the temperature of the blood entering the brain.

As the major arteries leave the circle of Willis they reduce their diameter to become arterioles and pial vessels. Pial arteries then plunge at a 90 degree angle into brain parenchyma. There is much evidence that there is a close relationship between pial vessels and the leptomeninges. These vessels, as they enter the parenchyma, are invested with a leptomeningeal sheath and are surrounded by a cerebrospinal fluid (CSF)-containing space. It should be mentioned that most studies of cerebral vessels using methods of staining and light microscopy have not shown differences between brain vessels and vessels in other organs.

Venous System

While the brain's arterial system is complicated, the configuration of the brain's venous system is even more complex and provides many opportunities for mixing of blood draining various brain regions (Fig. 1.2 [2]). Blood is drained from the brain via two primary sets of veins:

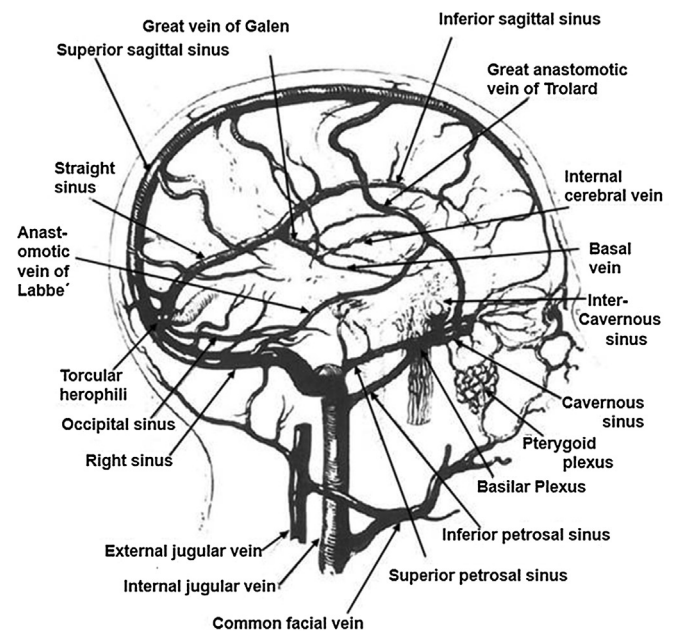


FIGURE 1.2 The brain venous system. Modified from Shenkin HA, Harmel MH, Kety SS. *Dynamic anatomy of the cerebral circulation*. *Arch Neurol Psychiat* 1948;60:240–52.

the external group and the deep or internal group. These drain into the dural sinuses and then the internal jugular veins. The external venous system is divided into the superior, middle, inferior, and occipital cerebral veins, which drain the outer portion of the cerebral hemispheres. The superior cerebral vein drains the cortex and underlying white matter above the corpus callosum. Several veins on each side merge to form three large trunks, which enter the superior sagittal sinus or straight sinus. The most prominent superior cerebral vein is the great anastomotic vein of Trolard connecting the superior sagittal sinus with the Sylvian vein. The internal cerebral or deep veins include a variety of small transcerebral veins draining the bulk of white matter from the anterior and middle group of the brain. This system eventually drains through the great vein of Galen and the straight sinus. The cerebellum is drained primarily by two sets of veins. The inferior cerebellar veins are larger and end in the transverse superior petrosal and occipital sinuses. The superior cerebellar veins are smaller and empty in part into transverse and superior petrosal sinuses and in part into the great vein of Galen and the straight sinus. The brain stem is drained by veins terminating in the inferior and transverse petrosal sinuses. Veins from all parts of the brain drain into many sinuses situated between two layers of dura, that is, superior sagittal sinus, inferior sagittal sinus, occipital sinus, superior petrosal sinus, cavernous sinus, and transverse sinus. Extensive inter-venous collateral anastomoses exist between the two main venous draining systems and with the extracranial venous draining system.

Capillary System

The brain contains a rich network of capillaries; however, the density of capillaries within the CNS is less than that in the heart, kidney, and muscle. Gray matter contains about 2½ times as many capillaries as does white matter; that is, cerebral cortex has about 1000 capillaries/mm³ and white matter about 300 capillaries/mm³. It has been proposed that capillary density is correlated with the number of synapses in a particular brain region. The high density of capillaries in the cervical sympathetic ganglion, which contains synapses, compared to that in the trigeminal ganglion, which lacks them, demonstrates this point. Oxygen consumption may be the link between capillary density and synaptic frequency. Support for this hypothesis comes from work demonstrating that glucose utilization of gray matter is greater than that of white matter by a factor similar to the ratio of capillary densities for the two tissues. Exposure of experimental animals to hypoxia for a long period leads to an increase in capillary density. Thus, a lack of oxygen must be either a direct or indirect stimulus to capillary growth; however, the precise mechanism responsible for this increased vascularity remains unknown. Cerebral capillary density also varies with age and it has been demonstrated that capillary density at birth is about 30% of that in the adult and is even lower in the premature infant.

Blood–Brain Barrier and Capillary Permeability

The concept of a blood–brain barrier (BBB) arose from the work of a number of investigators who demonstrated that certain dyes and pharmacologically active compounds did not enter the brain but could enter most other organs. The barrier had to be a vascular one because the same substances would readily enter the brain when injected directly into the CSF. It was subsequently shown that the dyes that could not penetrate the brain from the vascular side were bound to plasma proteins, so that the barrier was actually dye–protein complexes. Morphological localization of the barrier to circulating protein has been shown using horseradish peroxidase, a protein that could be localized by electron microscopy [3].

The BBB separates two of the major compartments of the CNS, the brain and CSF, from the third compartment, the blood. The sites of the barrier are the interfaces between the blood and these two compartments: the choroid plexus, the blood vessels of the brain and subarachnoid space, and the arachnoid membrane. All BBB sites are characterized by cells connected by tight junctions, which restrict intercellular diffusion. These cells are represented by endothelia of blood vessels, epithelia of the

choroid plexus, and cells of the arachnoid layer. When cells are connected via tight junctions, they act as if they were one single layer of cells and solute exchange occurs transcellularly. These cells thus determine the solubility and transport functions of the entire layer of cells. Lipid-soluble substances penetrate easily and equilibrate between brain and blood quickly. There is only minimal transport by pinocytotic vessels at the barrier site, and this in addition to the tight junctions limits protein transport into the extracellular fluid.

While passage of more permeable substances (sugars and amino acids) into brain is determined by both CBF and permeability characteristics, the permeability of ions and large molecules depends largely on the characteristics of the BBB membrane rather than blood flow. Nonelectrolytes of small molecular weight penetrate faster than their lipid solubilities and diffusion coefficients would predict. Thus, the presence of water channels across the barrier is likely. The BBB may not be equally permeable in all areas of the brain. For example, area postrema, choroid plexus, hypophysis, pineal, and areas in the hypothalamus have no BBB at all. In these areas cerebral capillaries have fenestrations, and there are a large number of pinocytotic vesicles in the endothelial cells. Besides these areas, within brain there are moderate differences in barrier permeability in different regions. The entry of most solutes into gray matter is about three to four times faster than into white matter. This may be correlated with a similar difference in the length of capillaries per unit volume of gray compared to white matter.

Breakdown of the BBB can be caused by mechanisms that either alters the tension in the walls of small vessels or damage the vessel wall in other ways, that is, chemically or by radiation. Several investigators have shown that inhalation of a high concentration of CO₂ (20%) increases the penetration of labeled proteins into the brain. The effect of CO₂ on BBB permeability is reversible. Repeated seizure activity also gives rise to extreme cerebral vasodilation, and again the barrier may be opened. As with CO₂ administration BBB breakdown is enhanced by elevated blood pressure. In a classic article, Rapoport et al. [4] characterized the properties of osmotic opening of the barrier. The degree of opening was determined by the amount of extravasation of dye (Evan's blue) as hyperosmolar solutions of different concentrations were applied to the surface of the cerebral cortex. The conclusions of their study were that barrier opening was reversible and that the degree of opening increased with increased osmolality. They suggested that hyperosmolar solutions shrink endothelial cells and open the tight junctions. However, it has also been suggested that hyperosmolar solutions increase vesicular transport in endothelial cells.

The structural integrity of cerebral endothelium is dependent on metabolism, and endothelia resist hypoxia

and ischemia much longer than do other cells of the brain. It has been shown that barrier impermeability to dye is retained for up to 12h after an animal is killed. However, histochemical and biochemical studies have shown that cerebral cortical neurons do not survive O₂ deprivation for more than 3–8min. Following occlusion of the blood supply to a region of brain, cerebral endothelial cells swell or flatten, but endothelium continuity is undisturbed. Vascular disruption develops after several hours and is preceded by irreversible metabolic and cytological changes in cells of the surrounding parenchyma. Thus, hypoxia and ischemia are not potent causes of BBB breakdown. A large number of other miscellaneous insults may increase barrier permeability. These include physical, chemical, infective, allergic, and neoplastic processes, and they generally result in barrier opening by sensitizing or damaging directly cerebral blood vessels.

OVERVIEW OF CEREBRAL HEMODYNAMICS

The brain's function and survival is dependent on providing it with oxygen and energy-producing substrates. In order to fulfill its needs, this complex neuronal system uses a significant portion of total body blood flow (about 15–20% of cardiac output) and consumes roughly a quarter of resting total body oxygen consumption. This section briefly reviews the hemodynamic principles which determine CBF and cerebrovascular resistance (CVR) and emphasizes mechanical control mechanisms within the macrocirculation of the brain.

General Hemodynamic Principles

Hemodynamics can be defined as the physical factors that govern blood flow. The physical laws formulated to describe laminar flow of fluids through nondistensible tubes are helpful in understanding in vivo cerebrovascular macrohemodynamics. These are the same physical factors that govern the flow of any fluid, and are based on a fundamental law of physics, namely Ohm's law, which states that current equals the voltage difference divided by resistance. In relating Ohm's law to fluid flow, the voltage difference is the pressure difference (ΔP ; sometimes called driving pressure, perfusion pressure, or pressure gradient), the resistance is the resistance to flow (R) offered by the blood vessel and its interactions with flowing blood, and the current is the blood flow. This hemodynamic relationship can be summarized by:

$$Q = \frac{\Delta P}{R} = \frac{(P_A - P_V)}{R} \quad (1.1)$$

For the flow of blood in a blood vessel, ΔP is the pressure difference between any two points along a given length of the vessel. When describing the flow of blood for an organ, the pressure difference is generally considered to be the difference between arterial pressure (P_A) and venous pressure (P_V). For example, in brain, cerebral perfusion pressure (CPP), the difference between arterial inflow and downstream outflow pressure (ΔP), is used as the relevant driving pressure for CBF. CPP is the difference between intraarterial pressure and the pressure in the thin-walled cerebral veins, collapsible at the point of entry into the venous sinuses. Cerebral venous pressure changes in parallel with intracranial pressure (ICP), and is normally 2–5mmHg higher than ICP. Therefore, the driving pressure in brain is calculated as the difference between mean arterial blood pressure (MAP) and cerebral venous pressure or ICP, whichever is higher. Resistance is determined principally by vessel radius and can be calculated from Eq. (1.1) to estimate total CVR or resistance of any vascular segment of interest in which flow and upstream and downstream pressure gradients are known.

Under ideal laminar flow conditions, in which vascular resistance is independent of flow and pressure, the relationship between pressure, flow, and resistance can be depicted as shown in Fig. 1.3. Because flow and resistance are reciprocally related, an increase in resistance decreases flow at any given ΔP . Also, at any given flow along a blood vessel an increase in resistance increases ΔP . Changes in resistance are the primary means by which blood flow is regulated within organs because control mechanisms in the body generally maintain arterial and venous blood pressures within a narrow range. However, changes in perfusion pressure, will affect flow. The above relationship also indicates that there is a linear and proportionate relationship between flow and perfusion pressure. This linear relationship, however, is not followed when pathological conditions lead to turbulent

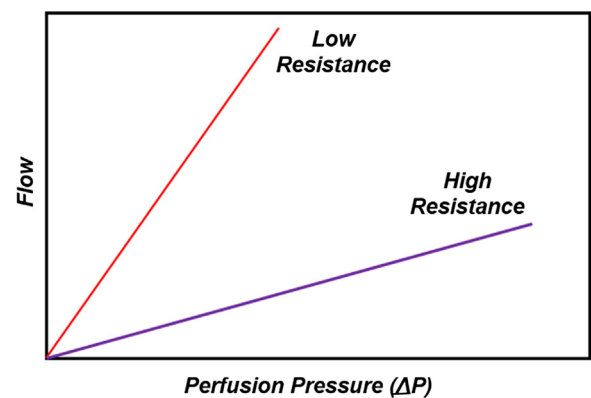


FIGURE 1.3 Pressure, flow, and resistance relationship.

flow, because turbulence decreases flow at any given perfusion pressure. Furthermore, the pulsatile nature of flow in large arteries alters this relationship so that greater pressures are required for a given flow. In other words, pulsatility, like turbulence, increases resistance to flow.

There are three primary factors that determine the resistance to blood flow within a single vessel: vessel diameter (or radius), vessel length, and blood viscosity—the most important, quantitatively and physiologically, being vessel diameter. The reason for this is that vessel diameter changes because of contraction and relaxation of vascular smooth muscle in the wall of the blood vessel. Furthermore, as discussed in the following, very small changes in vessel diameter lead to large changes in resistance. Vessel length does not change significantly and blood viscosity normally stays within a small range, except when hematocrit changes. The flow of fluids through blood vessels (tubes) can be described by Poiseuille's law (Fig. 1.4),

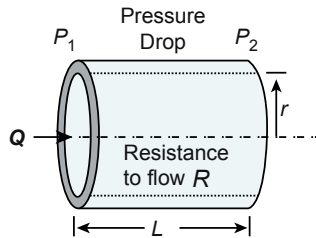


FIGURE 1.4 Depiction of Poiseuille's law.

$$Q = \frac{\Delta P \cdot r^4}{\eta \cdot L} \quad (1.2)$$

which shows that the major determinants of CBF (Q) are perfusion pressure (ΔP), blood viscosity (η), vessel radius (r), and vessel length (L).

Blood vessel resistance (R) is directly proportional to the length (L) of the vessel and the viscosity (η) of the blood, and inversely proportional to the radius of the vessel to the fourth power (r):

$$R = \frac{\eta \cdot L}{r^4} \quad (1.3)$$

Thus, a vessel having twice the length of another vessel (and each having the same radius) will have twice the resistance to flow. Similarly, if the viscosity of the blood increases twofold, the resistance to flow will increase twofold. In contrast, an increase in radius will reduce resistance.

Furthermore, the change in radius alters resistance to the fourth power of the change in radius (Fig. 1.5). For example, a twofold increase in radius decreases resistance by 16-fold! Therefore, vessel resistance is

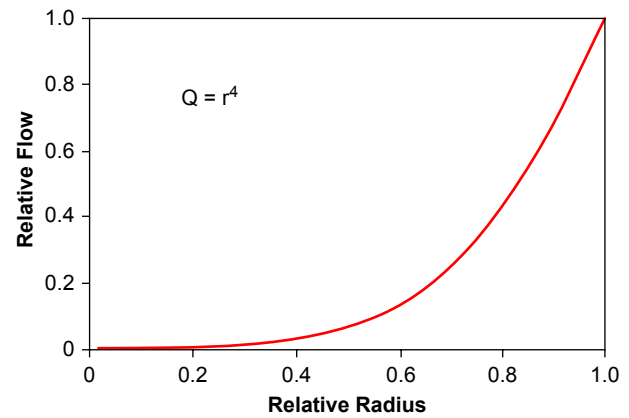


FIGURE 1.5 Relationship between flow and vessel radius to the fourth power (assumes constant ΔP , L , η , and laminar flow).

exquisitely sensitive to changes in radius of the vessel. It is by this mechanism that CVR can change rapidly, and dramatically alter regional or global CBF during normal or pathophysiological conditions. The stability of CBF (cerebral autoregulation) is achieved via the fine tuning of vessel diameter in response to fluctuations in perfusion pressure. The major cerebral and pial arteries are located outside the brain parenchyma and are surrounded anatomically by displaceable CSF, which maximizes the arteries' ability to widely change diameter and geometry. Intracerebral vessels, however, are constrained by extravascular tissue and structural elements.

Blood viscosity is the thickness and stickiness of blood, and it is a direct measure of the resistance of blood to flow through vessels. The primary determinants of blood viscosity are hematocrit, red cell deformability, red blood cell aggregation, and plasma viscosity. Viscosity (internal frictional resistance) of the transported fluid is often overlooked in predicting CBF because direct measurement is uncommon. Importantly, viscosity varies directly with hematocrit and any increase in the aggregation state of blood cellular components. Because blood viscosity also varies inversely with shear rate (i.e., is a non-Newtonian fluid), Poiseuille's law does not precisely describe the relationship between CBF and viscosity, particularly in the microcirculation [5]. Shear rate, a parameter that describes the velocity gradient of laminar blood flow through a vessel, is inversely proportional to vessel radius. Therefore, for a given blood velocity, shear rates are greater in small vessels than in larger vessels ($300\text{--}500\text{ s}^{-1}$ in arterioles vs. 50 s^{-1} in aorta) [6], and apparent viscosity is thus lower in the microcirculation. The latter effect is the well-known Fahraeus–Lindqvist effect and predicts that viscosity is reduced by about 5% at $300\text{ }\mu\text{m}$ diameters and by 50% at $20\text{ }\mu\text{m}$ diameters relative to large bore tubes [6]. There has been some controversy concerning the effects of blood viscosity on CBF. Some

investigators have shown that changes in viscosity alters CBF [7], whereas others have found that changes in viscosity are counteracted by compensatory vascular responses of the cerebral microcirculation, resulting in a well-maintained CBF [8]. It is likely that an increased viscosity is compensated by vasodilation to keep CBF unchanged. Conversely, CBF may be decreased by an increased viscosity when the vasodilatory capacity of the vessels is exhausted.

Segmental Vascular Resistance

The principal regulation and major source of vascular resistance within the cerebral circulation was always thought to be at the arteriolar level, as predicted by Poiseuille's law. However, data from experiments in which the pressure gradient was measured directly across different segments of the vascular bed indicate that the large extracranial vessels (internal carotid and vertebral arteries) and intracranial pial vessels contribute roughly 50% of total CVR (Table 1.1 [9]). The unusually prominent vasoregulatory role of large cerebral arteries may serve to equalize flow during focal neuronal activity and dampen pressure fluctuations in downstream vascular beds, for example, mitigating changes in microvascular pressure during systemic hypertension or hypotension.

Pressure–Volume Relationships

The vascular network of the brain is contained within a rigid bony structure and membranous dura

TABLE 1.1 Distribution of Segmental Vascular Resistance in Cerebral Circulation

Species	Segment	Percentage of Total
Dog	Aorta to 250- to 400- μm pial arteries	10
	Aorta to circle of Willis	22–31
Rhesus monkey	Aorta to 250- to 400- μm pial arteries	13
Cat	Aorta to 200- to 455- μm pial arteries	39
	Aorta to 250- to 455- μm pial arteries	10
	200- to 455- μm pial arteries to 25- to 40- μm	39
	Aorta to 30- to 40- μm pial arterioles	17
	Circle of Willis to 150- to 200- μm pial arteries	26
	Aorta to 150- to 250- μm pial arteries	51

Permission from Heistad DD, Kontos HA. Cerebral circulation. In: Berne RM, Sperelakis N, editors. *Handbook of physiology: the cardiovascular system III*. Bethesda American Physiological Society; 1978. p. 137–82.

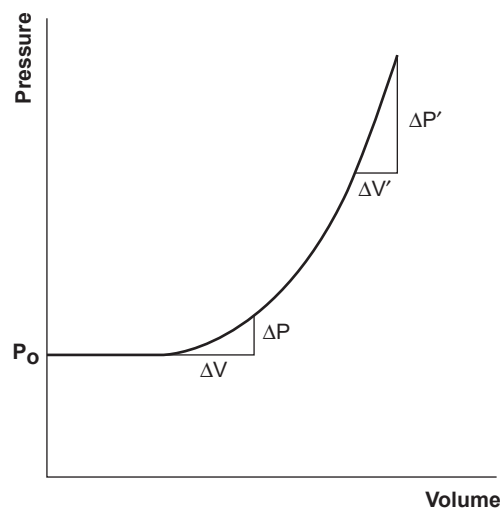


FIGURE 1.6 Pressure–volume relationship (idealized) in brain. An initial increase in volume of the cranial space (ΔV) produces an increase in ICP (ΔP). As the curve steepens (in intracranial hypertension), subsequent increases in volume generate exponentially larger increases in ICP.

with a fixed volume and a limited potential for external, vented release of intracranial contents. Therefore, extravascular pressure is critically important in cerebrovascular hemodynamics because arterial transmural pressure (difference between intraarterial and extravascular pressures) is equivalent to ICP. Under normal conditions, ICP is less than 15 mmHg and reflects the volume of three compartments: brain parenchyma (1200–1600 mL in the adult human), extracellular/CSF (100–150 mL) and intravascular blood (100–150 mL). Because the intracranial vault is fixed in volume, increases in the size of one compartment must be compensated by removal of an equivalent amount of another compartment, or ICP will increase. This pressure–volume relationship is exponential (Fig. 1.6), and the point at which perfusion-compromising ICP elevation occurs is dependent on brain elastance and potential displacement of intracranial contents (CSF displacement).

Cerebral Blood Volume

Intracranial blood volume is determined by two factors, CBF and capacitance vessel diameter (small veins and venules). Cerebral blood volume (CBV) increases with vasodilation and will decrease with vasoconstriction. Although CBF frequently changes in the same direction as CBV, these variables are inversely related under some normal (autoregulation) or pathological conditions. Further, CBV is not equally distributed throughout brain; blood volume per unit weight is greater in gray than in white matter with further variation among the various nuclei. Average CBV in humans is 3–4 mL/100 g

tissue. Pathology that affects either CBF or cerebral venous capacitance may modulate CBV with subsequent effects on ICP. More quantitatively, the central volume principle [10] relates the volume that intravascular blood occupies within brain (CBV in mL) and the volume of blood that moves through the brain per unit time (CBF in mL/min):

$$Q = \text{CBV}/t \quad (1.4)$$

Change in vascular diameter will directly affect CBV but not necessarily CBF when mean transit time (t) is simultaneously altered. For example, although CBV is increased during vasodilation, CBF may not change if blood flow velocity is correspondingly reduced. Surplus CBV accumulates primarily within cerebral veins, known to receive sympathetic innervation and to respond to sympathetic stimulation, and within capillaries to a smaller degree. Normally, increases in CBV can be physiologically controlled by two maneuvers: (1) increased blood outflow of the extracranial venous circulation and (2) restricted inflow via constriction of the major feeding arteries.

Pressure–Flow Relationships

The ability of CBF to remain constant despite changes in blood pressure (i.e., CPP) is referred to as cerebral autoregulation [11,12]. Autoregulation has been well demonstrated in both animals and humans. It has also been shown to be impaired or completely abolished during hypoxemia or hypercapnia. In healthy brain, arterial diameter increases or decreases within 30s to 2min in order to actively control CBF and maintain flow constant over a range of CPP (about between 60 and 160mmHg) (Fig. 1.7). Within the

autoregulatory range, CBF remains constant via cerebral vasoconstriction when CPP increases or vasodilation when CPP decreases. Below the autoregulatory range (60mm Hg–“lower limit”) a decrease in CPP decreases CBF. Above the “upper limit” (160mmHg) an increase in CPP increases CBF. Individuals with chronic hypotension demonstrate a leftward shift of the autoregulation curve, while chronic hypertension shifts the curve to the right. In neonates or infants, there is some question regarding the upper and lower limits of autoregulation because MAP in this age group is below 60mmHg. Systolic pressures of from 41 to 70mmHg have been reported in normal newborns and these values are close to the lower limit of autoregulation in adults. Furthermore, MAP above 60mmHg does not appear to be common until the end of the first year of life. In addition, in the premature infant, arterial blood pressure has been reported to be in the range of 64/39mmHg. Thus, it appears that the neonate and infant exhibit autoregulation; however, the critical CPP may be around 40mmHg instead of 60mmHg as in adults. Autoregulation may be abnormal or lacking in injured brain.

Autoregulatory limits have been extensively studied [11] and values vary in animals and humans. The upper and lower limit of autoregulation has been defined by numerous criteria: the CPP where the first significant change in CBF occurs; the pressure at which no further change in CVR is observed; or by direct observation to determine the pressure at which maximum vessel diameter is reached. While concern about CPP generally focuses on hypotension, it has been shown that with hypertension there is an “escape” (upper limit) from autoregulation such that CBF varies directly with CPP. The level of hypertension above which there is escape from autoregulation is in the range of 150–170mmHg. It is unclear if this escape occurs in fetuses or newborns, or at which pressure levels. Furthermore, the mechanism accounting for autoregulation remains in debate despite many years of study, with data available to support both the myogenic and metabolic hypothesis [13,14].

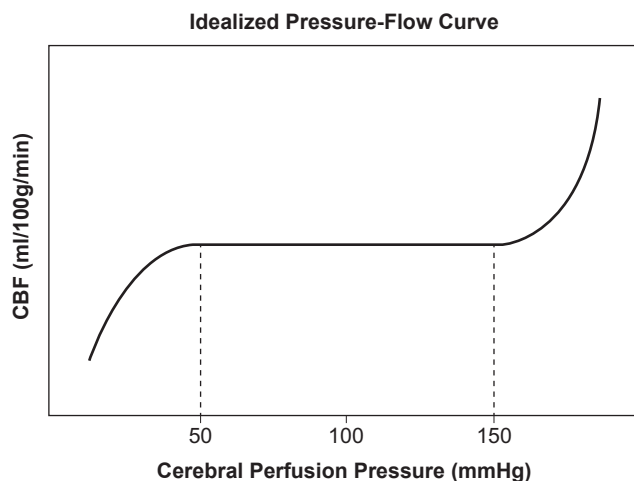


FIGURE 1.7 Idealized autoregulatory curve. The lower and upper limits or “breakpoints” are indicated by dotted lines, beyond which CBF varies as a function of CPP.

CONCLUSION

Application of general hemodynamic principles and an appreciation for the complicated anatomical vascular system in brain, offers an initial understanding of CBF, mechanical control of cerebral macro- and microcirculation, and the basis for understanding CBF in cerebrovascular disease. Pressure–volume and pressure–flow relationships have been well characterized in brain, although the mechanisms controlling these relationships remain of interest and controversial.

References

- [1] Chusid JG. Correlative neuroanatomy and functional neurology. 14th ed. Los Altos (CA): Lange Medical Publishers; 1970.
- [2] Shenkin HA, Harmel MH, Kety SS. Dynamic anatomy of the cerebral circulation. *Arch Neurol Psychiatry* 1948;60:240–52.
- [3] Reese TS, Karnovsky MJ. Fine structural localization of a blood–brain barrier to exogenous peroxidase. *J Cell Biol* 1967;34:207–17.
- [4] Rapoport SI, Hori M, Klatzo I. Testing a hypothesis for osmotic opening of the blood–brain barrier. *Am J Physiol* 1972;223:323–31.
- [5] Hurn PD, Traystman RJ, Shoukas AA, Jones MD. Pial microvascular hemodynamics in anemia. *Am J Physiol* 1993;264:H2131–5.
- [6] Milnor WR. Hemodynamics. 2nd ed. Baltimore: Williams and Wilkins; 1989. p. 11–57.
- [7] Massik J, Tang YL, Hudak ML, Koehler RC, Traystman RJ, Jones Jr MD. Effect of hematocrit on cerebral blood flow with induced polycythemia. *J Appl Physiol* 1987;62:1090–6.
- [8] Hudak ML, Jones Jr MD, Popal AS, Koehler RC, Traystman RJ, Zeger S. Hemodilution causes size-dependent constriction of pial arterioles in the cat. *Am J Physiol* 1989;257:H912–7.
- [9] Heistad DD, Kontos HA. Cerebral circulation. In: Berne RM, Sperelakis N, editors. *Handbook of physiology: the cardiovascular system III*. Bethesda American Physiological Society; 1978. p. 137–82.
- [10] Meier P, Zierler KL. On the theory of the indicator-dilution method for measurement of blood flow and volume. *J Appl Physiol* 1954;6:731–44.
- [11] Traystman RJ. Microcirculation of the brain. In: Mortillaro NA, editor. *The physiology and pharmacology of the microcirculation*. San Diego: Academic Press; 1983. p. 237–98.
- [12] Rapela CE, Green HD. Autoregulation of canine cerebral blood flow. *Circ Res* 1964;15:205–11.
- [13] McPherson RW, Koehler RC, Traystman RJ. Effect of jugular venous pressure on cerebral autoregulation in dogs. *Am J Physiol* 1988;255:H1516–24.
- [14] Paulson OB, Strandgaard S, Edvinsson L. Cerebral autoregulation. *Cerebrovasc Brain Metab Rev* 1990;2:161–92.

CHAPTER

2

Cerebral Microcirculation

T. Dalkara

Hacettepe University, Ankara, Turkey

INTRODUCTION

Research on microcirculation has led to an unprecedented progress with help of amazing developments in imaging technology. It is now possible to image capillaries with high resolution down to the depths of cortex, measure O₂ saturation and tension in them, track fast erythrocyte movements, and study Ca²⁺ signaling, vascular diameter changes, and neurovascular coupling in wild-type as well transgenic animals expressing a large variety of reporter or actuator proteins. Not unexpectedly, it emerges that microvasculature is a complex system evolved to optimally deliver O₂, glucose, and other nutrients to match the local need of the surrounding tissue. Its function is regulated by even more complex mechanisms. This progress has been complemented with discovery of surprisingly important roles

of microcirculation in brain diseases. The present review will briefly outline some of these developments primarily in the context of stroke and microvascular dysfunction.

ANATOMY AND PHYSIOLOGY OF MICROCIRCULATION

Several arteries penetrate into the brain tissue after originating from the pial arterial/arteriolar network covering the brain surface. The penetrating arteries branch into arterioles and then to a network of capillaries. CNS capillaries are composed of a single layer of endothelium surrounded by a continuous basement membrane and are covered by astrocyte end feet over the abluminal wall (Fig. 2.1). Endothelial cells are connected by tight junction proteins and form the blood–brain barrier

References

- [1] Chusid JG. Correlative neuroanatomy and functional neurology. 14th ed. Los Altos (CA): Lange Medical Publishers; 1970.
- [2] Shenkin HA, Harmel MH, Kety SS. Dynamic anatomy of the cerebral circulation. *Arch Neurol Psychiatry* 1948;60:240–52.
- [3] Reese TS, Karnovsky MJ. Fine structural localization of a blood–brain barrier to exogenous peroxidase. *J Cell Biol* 1967;34:207–17.
- [4] Rapoport SI, Hori M, Klatzo I. Testing a hypothesis for osmotic opening of the blood–brain barrier. *Am J Physiol* 1972;223:323–31.
- [5] Hurn PD, Traystman RJ, Shoukas AA, Jones MD. Pial microvascular hemodynamics in anemia. *Am J Physiol* 1993;264:H2131–5.
- [6] Milnor WR. Hemodynamics. 2nd ed. Baltimore: Williams and Wilkins; 1989. p. 11–57.
- [7] Massik J, Tang YL, Hudak ML, Koehler RC, Traystman RJ, Jones Jr MD. Effect of hematocrit on cerebral blood flow with induced polycythemia. *J Appl Physiol* 1987;62:1090–6.
- [8] Hudak ML, Jones Jr MD, Popal AS, Koehler RC, Traystman RJ, Zeger S. Hemodilution causes size-dependent constriction of pial arterioles in the cat. *Am J Physiol* 1989;257:H912–7.
- [9] Heistad DD, Kontos HA. Cerebral circulation. In: Berne RM, Sperelakis N, editors. *Handbook of physiology: the cardiovascular system III*. Bethesda American Physiological Society; 1978. p. 137–82.
- [10] Meier P, Zierler KL. On the theory of the indicator-dilution method for measurement of blood flow and volume. *J Appl Physiol* 1954;6:731–44.
- [11] Traystman RJ. Microcirculation of the brain. In: Mortillaro NA, editor. *The physiology and pharmacology of the microcirculation*. San Diego: Academic Press; 1983. p. 237–98.
- [12] Rapela CE, Green HD. Autoregulation of canine cerebral blood flow. *Circ Res* 1964;15:205–11.
- [13] McPherson RW, Koehler RC, Traystman RJ. Effect of jugular venous pressure on cerebral autoregulation in dogs. *Am J Physiol* 1988;255:H1516–24.
- [14] Paulson OB, Strandgaard S, Edvinsson L. Cerebral autoregulation. *Cerebrovasc Brain Metab Rev* 1990;2:161–92.

CHAPTER

2

Cerebral Microcirculation

T. Dalkara

Hacettepe University, Ankara, Turkey

INTRODUCTION

Research on microcirculation has led to an unprecedented progress with help of amazing developments in imaging technology. It is now possible to image capillaries with high resolution down to the depths of cortex, measure O₂ saturation and tension in them, track fast erythrocyte movements, and study Ca²⁺ signaling, vascular diameter changes, and neurovascular coupling in wild-type as well transgenic animals expressing a large variety of reporter or actuator proteins. Not unexpectedly, it emerges that microvasculature is a complex system evolved to optimally deliver O₂, glucose, and other nutrients to match the local need of the surrounding tissue. Its function is regulated by even more complex mechanisms. This progress has been complemented with discovery of surprisingly important roles

of microcirculation in brain diseases. The present review will briefly outline some of these developments primarily in the context of stroke and microvascular dysfunction.

ANATOMY AND PHYSIOLOGY OF MICROCIRCULATION

Several arteries penetrate into the brain tissue after originating from the pial arterial/arteriolar network covering the brain surface. The penetrating arteries branch into arterioles and then to a network of capillaries. CNS capillaries are composed of a single layer of endothelium surrounded by a continuous basement membrane and are covered by astrocyte end feet over the abluminal wall (Fig. 2.1). Endothelial cells are connected by tight junction proteins and form the blood–brain barrier

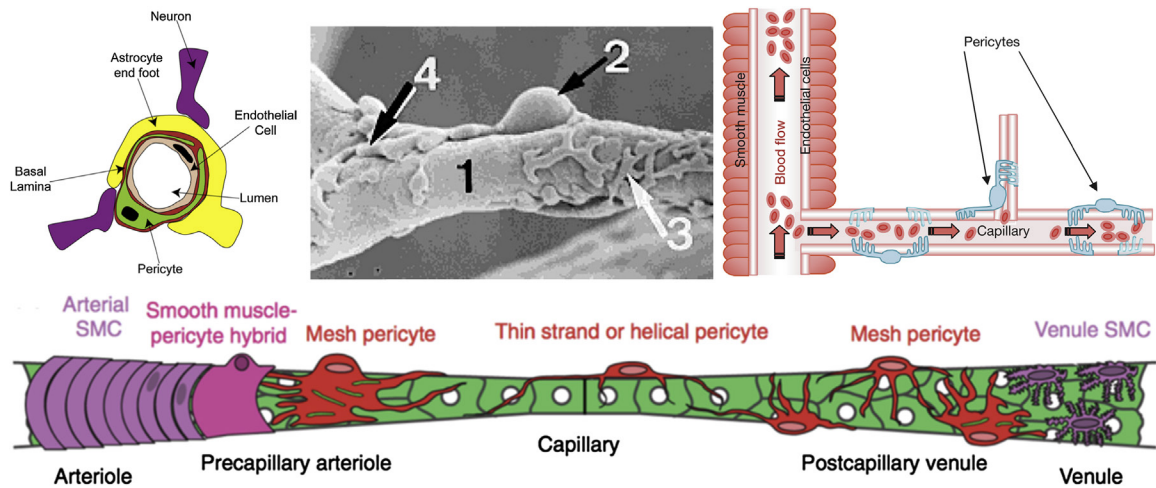


FIGURE 2.1 (Left) Schematic illustrating a capillary. Pericytes are located outside the endothelial cells and are separated from them and the parenchyma by a layer of basal lamina. In the parenchyma, astrocyte end feet and neuronal terminals are closely associated with the capillary. (Middle) Scanning micrograph of a vascular cast of a cortical capillary (1) with a pericyte-like structure (2) having primary and secondary processes (3) distributed around the vascular cast and the capillary branching points (4). (Right) Potential blood flow control sites in cerebral vasculature: arteriolar smooth muscle and pericytes placed especially on first-order capillaries and branching points. (Lower row) Schematic showing the continuum of mural cell types along the cerebral vasculature. SMC, smooth muscle cell. *Reproduced with permission from (left) Hamilton NB, Attwell D, Hall CN. Pericyte-mediated regulation of capillary diameter: a component of neurovascular coupling in health and disease. Front Neuroenergetics 2010;2; (middle) Rodriguez-Baeza A, et al. Anatomical Rec 1998;252:176–84; (right) Peppiatt CM, et al. Nature 2006;443:700–4; (lower row) Hartmann DA, Underly RG, Grant RI, Watson AN, Lindner V, Shih AY. Pericyte structure and distribution in the cerebral cortex revealed by high-resolution imaging of transgenic mice. Neurophotonics 2015;2:041402.*

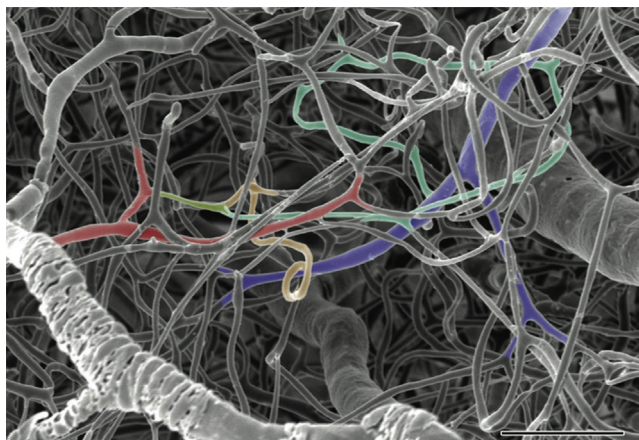


FIGURE 2.2 Corrosion cast scanning electron micrograph of the capillary plexus in chinchilla auditory cortex. Several interconnected capillary loops between a precapillary arteriole (red) and postcapillary venule (purple) are illustrated in different colors. Bar = 50 μm . *Reproduced with permission from Harrison RV, et al. Cereb Cortex 2002;12:225–33.*

(BBB), limiting and regulating the access of solutes to the CNS. Smooth muscle cells on arterioles are replaced by pericytes positioned between the two layers of basement membrane on capillaries [1,2]. The capillary density varies to match the regional metabolic demand and is correlated with synaptic density; hence, it is higher in the cortex than in the subcortical areas. It is estimated that the mean capillary size in human cortex is 6.5 μm in diameter and 53.0 μm in length. CNS capillaries form interconnected loops to adequately supply the tissue by passive O_2 diffusion (Fig. 2.2). Capillaries are not found

around large vessels (Pfeifer space); this area is directly oxygenated by diffusion of O_2 from the large vessel (Krogh tissue cylinder) [3]. Studies in the intact mouse brain show that, during baseline activity, arterioles provide 50% of the total extracted O_2 , whereas the majority of the remaining O_2 is extracted from the first few capillary branches, which is followed by recruitment of high-branching-order capillaries during activation [3]. It should be noted that capillary segments are not linearly aligned but form loops that bring low- and high-branching-order segments in proximity such that their supply territories can interact [3] (Fig. 2.2).

The pressure gradient between the arterial and venous sides drives the microcirculatory flow. The venous out-flow pressure is in equilibrium with the intracranial pressure. Accordingly, microcirculatory flow and tissue oxygenation can be adversely affected by high intracranial pressure as well as reduced arterial pressure. All cerebral capillaries are perfused by red blood cells (RBCs) and plasma under physiological conditions. The RBC velocity in capillaries is highly variable (around 0.2–4.4 mm/s). Random variations in RBC velocity including occasional stalls are observed in experimental animals under resting conditions. Capillary transit times of RBCs therefore significantly vary between neighboring branches of the network. A high capillary transit time heterogeneity (CTH) decreases the efficiency of O_2 transfer from RBCs [4]. The variability in transit times is reduced on neuronal activation, allowing more O_2 to be extracted. Although debated, it appears so that, to match the very focal demand by a small group of nearby

cells, the cerebral microvascular blood flow requires a final step of regulation after the arterioles, which serve a larger cohort of cells [1,4]. In addition to the enhanced perfusion in dilated arterioles during neuronal activity, pericyte relaxation as well as the vasodilatory stimulus provided by ATP released from shear-stressed RBCs may reduce the microvascular resistance and promote the RBC transit. Also, the capillary endothelial surface is covered by a 0.5- μm -thick glycocalyx that facilitates the passage of blood cells and, when damaged, disrupts capillary flow.

Pericytes express several vasoactive receptors, suggesting that they have the capacity to respond to neurotransmitters and vasoactive mediators released from nearby neurons and astrocytes. Indeed, *in vivo* studies with two-photon microscopy have shown that cortical capillaries dilated about 1 s before arterioles during sensory stimulation in mice under anesthesia, supporting the view that capillaries may play a direct role in flow regulation [5]. Capillary endothelia, pericytes communicating with them, and astrocyte end-feet surrounding capillaries can transmit dilatory signals to the upstream arteriole through gap junctions between them to promote arteriolar dilation for providing the blood volume increase in microcirculation [2].

NEUROVASCULAR UNIT AND COUPLING

An increase in neuronal activity leads to an enhanced blood flow to the active brain area (functional hyperemia). In addition to the vasodilation caused by adenosine and lactate produced during metabolic activity [6], the coupling of the blood flow with activity is orchestrated by the neurovascular unit, which is composed of the endothelia, pericytes, astrocyte end-feet, and terminals of the vasoregulatory nerves at the microcirculatory level [2,6] (Fig. 2.1).

Local interneurons or projections of the subcortical and brainstem nuclei terminate in the vicinity of microvessels or on astrocyte end feet around the vessels without making direct synaptic contacts [7]. The subcortical projections promote more global flow changes (e.g., during attention), whereas excitatory or inhibitory interneurons integrate local neuronal activity and differentially contribute to neurovascular coupling by releasing their distinctive mediators. For example, activity-induced Ca^{2+} increase in neuronal NO synthase expressing GABAergic interneurons causes NO synthesis, which rapidly diffuses across plasma membranes and relaxes smooth muscle cells and pericytes on vasculature.

Astrocytes may also play a role in neurovascular coupling by monitoring the neuronal activity with

their perisynaptic end feet and translating this information as the vasoactive signals released from their perivascular end feet [6]. Moreover, Ca^{2+} increase in perivascular end feet may release K^+ through the large-conductance Ca^{2+} -activated K^+ channels, which initially induces vasodilation but then vasoconstriction with increasing concentrations of K^+ . However, the *in vivo* significance of these astrocytic mechanisms is currently being evaluated. Of note, relative contributions of the above-outlined pathways to the neurovascular coupling vary in different brain regions and also with the developmental stage, species, and activation pattern (quick, short lasting vs. sustained vasodilatory responses) and, most likely, with the segment of the vascular tree (e.g., the proximal penetrating arteries vs. distal capillary bed).

Interest in pericytes has started to disclose several important microvascular functions mediated by these long-neglected cells on the microvessel wall. Pericytes are located on precapillary arterioles, capillaries, and postcapillary venules [8] (Fig. 2.1). Unlike smooth muscle cells, pericytes have a prominent soma, protruding out from the vascular wall (bump on a log appearance) and are embedded within two layers of basement membrane [9]. Processes that originate from pericyte soma extend along and branch around the microvessels. Processes are more circumferential at the arteriole end of the microvascular bed and at downstream bifurcating points, more longitudinal in the middle of a capillary, and have a stellate morphology at the venule end of the microcirculation (Fig. 2.1). In accordance with a contractile, flow-regulating phenotype, pericytes with circumferential processes express smooth muscle α -actin. *In vitro* as well as *in vivo* studies have shown that microvascular pericytes contract or dilate in response to vasoactive mediators applied or to sensory stimulation [1,5]. Such flow regulation with fine spatial resolution at the microcirculatory level may be essential for the brain and retina. However, it should be noted that not all microvascular pericytes are contractile and the ratio of the contractile ones may vary with the species, tissue, and developmental stage, as well as along the arteriovenous axis [8,9].

A close communication between the endothelia, pericytes, and astrocytes is required for development and functioning of the neurovascular unit as well as the BBB. The microvascular pericyte density is the highest in the retina and CNS compared with peripheral vessels in line with their role in formation and maintenance of the blood-brain/retina barrier [9]. The surface area of the vascular wall covered by pericytes and the number of pericytes per endothelial cell are correlated with the permeability of capillaries. Accordingly, pericyte dysfunction as well as deficiency leads to a leaky BBB [9].

MICROCIRCULATION AFTER STROKE AND THROMBOLYSIS

The microvascular injury inflicted by ischemia/reperfusion plays a critical role in determining tissue survival after recanalization by inducing microcirculatory clogging (no reflow) and disrupting the BBB integrity [10]. Evidence from clinical trials show that recanalization does not always lead to reperfusion of the ischemic tissue in patients with stroke treated with tissue plasminogen activator or interventional methods [11]. Since current imaging techniques assess perfusion by measuring the plasma transit through the microcirculation, the current average rate of 26% likely underestimates the rate of incomplete reperfusion in the setting of satisfactory recanalization [11] because the plasma continues to flow at the periphery of the microvessel wall bypassing the RBCs entrapped within the narrowed lumen [10].

Starting 1 h after middle cerebral artery (MCA) occlusion in the mouse, some of the microvessels show constrictions (Fig. 2.3). Narrowed lumina are filled with entrapped erythrocytes, leukocytes, and fibrin-platelet deposits. Leukocytes also populate the postcapillary venules and adhere to their wall to enter the CNS. Reducing microvascular clogging by inhibiting oxygen/nitrogen radical production, leukocyte adherence, platelet activation, or fibrin-platelet interactions have been shown to restore microcirculation and improve stroke outcome in animal models. BBB-impermeable agents such as the endothelial NO synthase inhibitor (*L-N-5*-(1-iminoethyl)-ornithine) or adenosine (continuously released from circulating nanoparticles) reduces the microvascular clogging and infarct volume, suggesting that restoring microvascular patency alone can improve stroke outcome without direct parenchymal neuroprotection [10,12]. These observations support the view that the outcomes of recanalization therapies can be improved by promoting microcirculatory reflow and preventing BBB leakiness, hence, hemorrhagic conversion and vasogenic edema. They also point to the critical but partly neglected importance of the microcirculation in neuroprotection [13].

Narrowing of the microvessel lumen was generally attributed to external compression by swollen astrocyte

end feet and to endothelial cell edema. Pericytes on microvessels were reported to play an important role in incomplete microcirculatory reperfusion as some of them contracted during ischemia and remained contracted despite reopening of the occluded artery [10]. Even subtle decreases in microvessel radius caused by pericyte contractions can cause RBC entrapments because capillary luminal size hardly allows RBC passage [1,10]. Entrapped RBCs may also impede flow of other blood cells and promote platelet and fibrin aggregation. The contracted pericytes die in rigor along the course of ischemia, which may contribute to loss of the BBB integrity [5].

MICROVASCULAR DYSFUNCTION AND DEMENTIA

In light of the discoveries at the microcirculatory level, the vascular hypothesis of dementia has been rekindled [9,14]. Pathological examination of brain specimens of patients with Alzheimer disease has revealed a reduced microvascular density and several morphological alterations in capillaries. β -Amyloid accumulation on capillaries as well as within degenerating pericytes has also been reported. Based on these findings, the vascular hypothesis of Alzheimer disease posits that microvascular dysfunction may secondarily cause degeneration of nerve endings of the subcortical projections innervating the cortex and then retrograde death of subcortical neurons (e.g., cholinergic) [2,9,14]. Of note, several cerebrovascular risk factors such as aging, hypertension, and diabetes can impair microcirculation over the course of years.

CAPILLARY TRANSIT TIME HETEROGENEITY AS A MEASURE OF CAPILLARY DYSFUNCTION

Modeling studies imply that capillary dysfunction can cause tissue hypoxia/ischemia without the presence of a proximal occlusion limiting the blood supply [4,15]. These models predict that an increase in blood

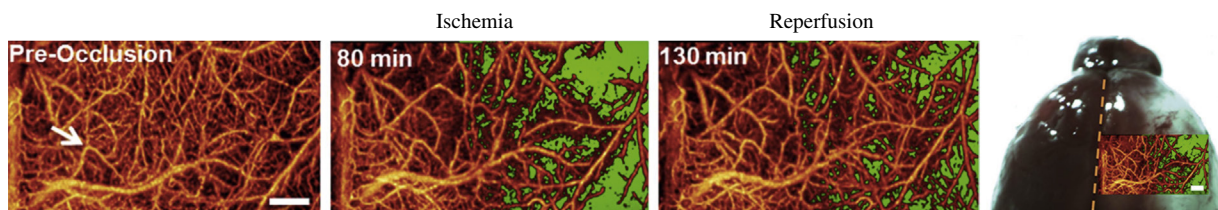


FIGURE 2.3 Incomplete microcirculatory reperfusion after 90 min of middle cerebral artery (MCA) occlusion. The *green area* depicts the lack of blood flow in the area of the MCA 80 min after occlusion and 130 min after reopening of the MCA as detected by optical microangiography. The image in the right is the optical microangiography image taken at 50 min of ischemia overlaid on the 24-h infarct analysis by histological staining as the area of pallor. Scale bar = 500 μ m. Reproduced with permission from Dziennis S, et al. *Sci Rep* 2015;5:10051.

flow can maintain tissue oxygenation when the capillary dysfunction (increased CTH) is mild. However, when CTH is further increased due to variable transit times through dysfunctional capillaries and accelerated transit from patent ones, neurovascular coupling mechanisms reduce the incoming blood flow to prevent functional shunting through patent capillaries because too rapid transit of RBCs drastically reduces O₂ extraction. In other words, to maintain tissue normoxia, neurovascular mechanisms reduce the blood flow rather than increasing it. Emerging evidence from asymptomatic apolipoprotein E (APOE) ε4 carriers supports these predictions; resting and activity-related CBF levels were found to be elevated in 19- to 28-year-old young carriers, whereas a long-term follow-up study of asymptomatic APOE ε4 carriers illustrated the transition from hyper- to hypoperfusion. The hypothesis that a high CTH could be a source of symptomatic tissue hypoxia has the potential to account for several other neurological conditions such as transient ischemic attacks without embolism, prolonged oligemia accompanying cortical spreading depression, stroke-like attacks in Cerebral Autosomal-Dominant Arteriopathy with Subcortical Infarcts and Leukoencephalopathy (CADASIL), and hyperperfusion after recanalization [15].

References

- [1] Hamilton NB, Attwell D, Hall CN. Pericyte-mediated regulation of capillary diameter: a component of neurovascular coupling in health and disease. *Front Neuroenergetics* 2010;2.
- [2] Iadecola C. Neurovascular regulation in the normal brain and in Alzheimer's disease. *Nat Rev Neurosci* 2004;5:347–60.
- [3] Sakadzic S, Mandeville ET, Gagnon L, et al. Large arteriolar component of oxygen delivery implies a safe margin of oxygen supply to cerebral tissue. *Nat Commun* 2014;5:5734.
- [4] Jespersen SN, Ostergaard L. The roles of cerebral blood flow, capillary transit time heterogeneity, and oxygen tension in brain oxygenation and metabolism. *J Cereb Blood Flow Metab* 2012;32:264–77.
- [5] Hall CN, Reynell C, Gesslein B, et al. Capillary pericytes regulate cerebral blood flow in health and disease. *Nature* 2014;508(7494):55–60.
- [6] Attwell D, Buchan AM, Charpak S, Lauritzen M, Macvicar BA, Newman EA. Glial and neuronal control of brain blood flow. *Nature* 2010;468(7321):232–43.
- [7] Cauli B, Hamel E. Revisiting the role of neurons in neurovascular coupling. *Front Neuroenergetics* 2010;2:9.
- [8] Hartmann DA, Underly RG, Grant RI, Watson AN, Lindner V, Shih AY. Pericyte structure and distribution in the cerebral cortex revealed by high-resolution imaging of transgenic mice. *Neurophotonics* 2015;2:041402.
- [9] Winkler EA, Bell RD, Zlokovic BV. Central nervous system pericytes in health and disease. *Nat Neurosci* 2011;14:1398–405.
- [10] Yemisci M, Gursoy-Ozdemir Y, Vural A, Can A, Topalkara K, Dalkara T. Pericyte contraction induced by oxidative-nitrative stress impairs capillary reflow despite successful opening of an occluded cerebral artery. *Nat Med* 2009;15:1031–7.
- [11] Dalkara T, Arsava EM. Can restoring incomplete microcirculatory reperfusion improve stroke outcome after thrombolysis? *J Cereb Blood Flow Metab* 2012;32:2091–9.
- [12] Gaudin A, Yemisci M, Eroglu H, et al. Squalenoyl adenosine nanoparticles provide neuroprotection after stroke and spinal cord injury. *Nat Nanotechnol* 2014;9(12):1054–62.
- [13] Gursoy-Ozdemir Y, Yemisci M, Dalkara T. Microvascular protection is essential for successful neuroprotection in stroke. *J Neurochem* 2012;123(Suppl. 2):2–11.
- [14] Iadecola C. The overlap between neurodegenerative and vascular factors in the pathogenesis of dementia. *Acta Neuropathol* 2010;120:287–96.
- [15] Ostergaard L, Jespersen SN, Engedahl T, et al. Capillary dysfunction: its detection and causative role in dementias and stroke. *Curr Neurol Neurosci Rep* 2015;15(6):37.

CHAPTER

3

The Glymphatic System and Brain Interstitial Fluid Homeostasis

J.J. Iliff^{1,2}, A.S. Thrane^{2,3}, M. Nedergaard^{2,4}

¹Oregon Health & Science University, Portland, OR, United States; ²University of Rochester Medical Center, Rochester, NY, United States; ³Haukeland University Hospital, Bergen, Norway; ⁴University of Copenhagen, Copenhagen, Denmark

INTRODUCTION

The maintenance of the interstitial compartment is a basic element of an organ's function that is of utmost importance in the brain, given neural cells' exquisite sensitivity to changes in their extracellular environment. In peripheral tissues, interstitial fluid (ISF) is formed from the filtration of plasma across the permeable capillary endothelium. Although a portion of the ISF is reabsorbed into postcapillary venules, much of the ISF and virtually all extracellular proteins are collected into primary lymphatic vessels, which return lymph fluid and proteins to the blood circulation. In the central nervous system (CNS), the presence of the blood–brain barrier (BBB), which restricts the filtration of water and proteins from the plasma, and the apparent absence of lymphatic vessels from brain tissues require that the “lymphatic” function of interstitial homeostasis be subserved by an alternative mechanism. In the CNS, the cerebrospinal fluid (CSF) circulation supports this function, serving as a sink and a crossroad for extracellular proteins and metabolites that cannot readily cross the BBB [1].

The exchange of ISF and CSF is a physiological process in the CNS that likely affects many aspects of brain function, including waste clearance, lipid metabolism, growth factor and neurohormone distribution, and immune surveillance. Dysfunction of these processes appears to contribute to the edema formation after cerebral ischemia and traumatic brain injury (TBI), to the accumulation of aggregated proteins in neurodegenerative conditions such as Alzheimer disease (AD), and to neuroinflammatory diseases such as multiple sclerosis [2].

INTERSTITIAL SOLUTE CLEARANCE

Under physiological conditions, the brain extracellular space comprises approximately 14–23% of the overall brain volume. ISF is formed from a combination of water crossing the BBB, water produced through cellular metabolism, and fluid from the CSF compartments. The relative contributions of these processes to ISF production is not clearly known, and may vary by brain region and physiological state. Interstitial solutes move through brain tissue both by the process of diffusion and bulk flow, with the relative contribution of each process being determined by the physical and chemical properties of the solute and the properties of the extracellular environment [3].

Diffusion and the Blood–Brain Barrier

Many interstitial solutes, including nonpolar molecules and those with specific BBB efflux transporters are readily cleared to the blood stream across the BBB. The process of diffusion, which is the movement of molecules down their concentration gradients driven by thermal motion, is very efficient on the microscopic scales of the brain microcirculation. Hence, the clearance of nonpolar molecules such as CO₂ and BBB efflux transporter substrates such as the drug verapamil (a substrate for P-glycoprotein) is diffusion limited [4]. Diffusion-limited clearance kinetics will be strongly influenced by molecular weight and the dimensions and nature of the extracellular space, with larger solutes moving more slowly than smaller, and with more rapid diffusion as the extracellular space becomes larger and less tortuous [3]. Beyond clearance of nonpolar

molecules and those with specific transporters at the BBB, diffusion also dominates the exchange of ISF and CSF in tissue closest to internal and external CSF compartments, including periventricular and subpial brain tissue (Fig. 3.1).

Bulk Flow and the Cerebrospinal Fluid Sink

The CSF compartment, either within the ventricles or the subarachnoid space, serves as a sink for interstitial solutes that cannot be cleared across the BBB. This process was initially thought to be driven solely by diffusion. However, as the inverse relationship between molecular mass and the rate of diffusion dictates, the exchange between most brain tissue and the nearest CSF compartment of larger molecules would be prohibitively slow. This becomes increasingly apparent as molecular masses approach macromolecular dimensions, such as the serum protein albumin (65 kD), which requires approximately 100 h to diffuse 1 cm within brain tissue. When inert solutes spanning more than two orders of magnitude of molecular mass that are not cleared across the BBB are injected into the brain, their clearance kinetics are virtually identical. For example, Groothuis et al.

demonstrated that sucrose [molecular weight (MW) 342 Da] and dextran-70 (MW 70,000 Da) are cleared from the rat brain with a half-life of 2.75 and 2.96 h, respectively [4]. This suggests that the clearance of interstitial solutes from the brain depends on bulk or convective flow of ISF, which was estimated by Cserr and colleagues in rats to be $0.11\text{--}0.29\ \mu\text{L}\cdot\text{g}^{-1}\cdot\text{min}^{-1}$, a value that is in line with the rate of lymph flow in peripheral organs [2].

Although these results have shown that bulk flow of ISF supports the clearance of interstitial solutes, several studies suggest that bulk flow is a feature of specific anatomical elements of brain tissue, rather than the wider ISF compartment. Tracers injected into brain tissue spread most rapidly along white matter tracks and along perivascular spaces surrounding cerebral blood vessels, but have a slower rate of spread through the bulk interstitium. This suggests that interstitial solute clearance may be driven by the combined actions of diffusion and bulk flow, with diffusion governing the microscopic movement of solutes between the interstitium and local perivascular spaces or white matter tracks, and bulk flow governing the macroscopic flux through brain tissue to distant CSF compartments (Fig. 3.1).

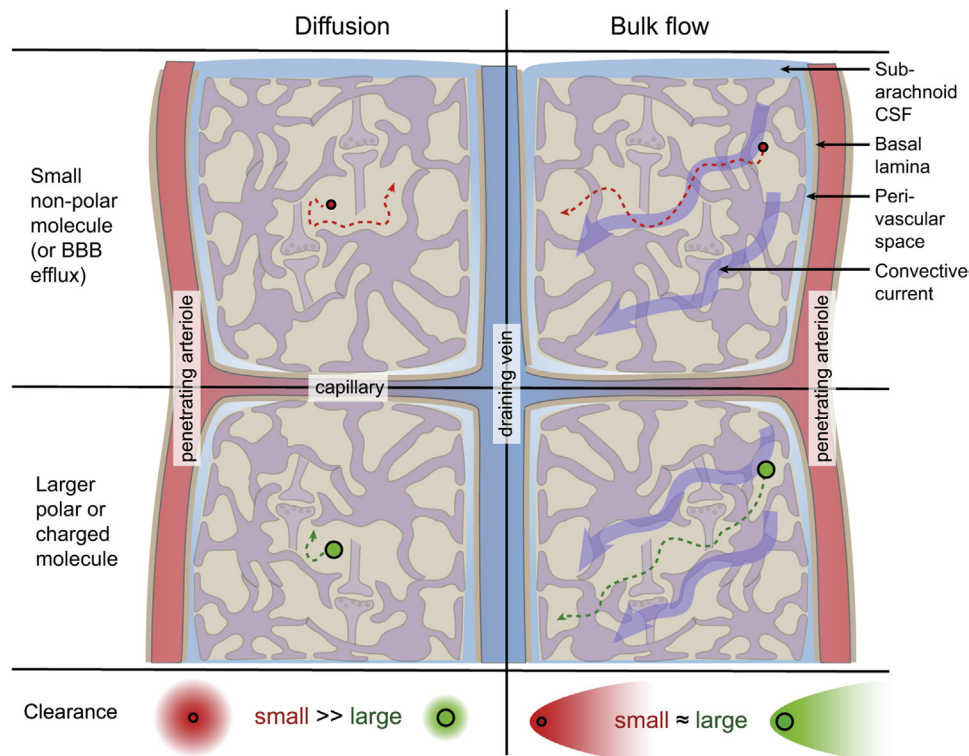


FIGURE 3.1 The contribution of diffusion and convection to the clearance of interstitial solutes from the brain parenchyma. Diffusion (left column) is a key driver of the clearance of small nonpolar molecules and those with specific blood–brain barrier (BBB) efflux transporters across the local BBB. The rate of diffusion is strongly influenced by molecular mass, with small molecules diffusing more rapidly than larger molecules. Bulk flow of brain interstitial fluid (right column) supports the clearance of solutes across long distances. Because interstitial fluid moves along with associated solutes, molecules are cleared by bulk flow at the same rate, independent of molecular size. CSF, cerebrospinal fluid.

PERIVASCULAR BULK FLOW AND THE GLYMPHATIC SYSTEM

Perivascular spaces surrounding cerebral blood vessels have long been known to facilitate the exchange of CSF and ISF. Although this process was generally held to occur slowly along the vasculature, a series of studies carried out in dogs and cats in the mid- to late 1980s suggested that the interaction of CSF and ISF along perivascular spaces was both rapid and polarized along the arterial and venous sides of the circulation, with CSF entering the brain along perivascular spaces surrounding penetrating cerebral arteries and ISF being cleared from the brain along perivascular spaces surrounding cerebral veins [1,2]. More recent studies have substantiated these findings employing dynamic imaging approaches in living animals rather than analysis of fixed or frozen tissues. In mice, *in vivo* two-photon microscopy demonstrated that fluorescent tracers injected into the subarachnoid CSF at the cisterna magna moved rapidly into and through the brain parenchyma along perivascular spaces surrounding cerebral arteries [5,6] (Fig. 3.2). Fluorescent tracers injected into the brain interstitium were in turn cleared along specific anatomical pathways including perivascular spaces surrounding large-caliber draining veins that drain to extraparenchymal venous sinuses, such as the internal cerebral veins that form the origin of the straight sinus. These findings have been confirmed both in rats and with brain-wide CSF tracer imaging using dynamic contrast-enhanced MRI. As detailed later, because perivascular bulk flow along this pathway depends on glial water transport, and because it assumes the lymphatic function of interstitial solute clearance, this brain-wide perivascular network has been termed the “glymphatic” system [6].

Anatomical Basis

Brain-wide imaging studies demonstrate that the CSF moving into the brain along perivascular spaces surrounding cerebral arteries originates within the basal cisterns along the conduit arteries of the circle of Willis, moves distally over the cortical surface along resistance vessels such as the middle cerebral arteries, and then enters the brain parenchyma along perivascular spaces surrounding penetrating cerebral arteries (Fig. 3.2A–C) [2,6]. Electron microscopy studies of the human leptomeningeal vasculature show that a layer of the pia mater invests leptomeningeal arteries and veins, forming a perivascular space, the Virchow–Robin space, that surrounds the elastic lamina of the arterial wall [1,2]. The pial investment of the leptomeningeal arteries follows the vessels as they penetrate the parenchyma, becoming fenestrated and discontinuous with increasing depth from the brain surface. In contrast, the pial investment

of the leptomeningeal veins reflects back upon the pia mater overlying the glia limitans, leaving perivascular spaces surrounding cerebral veins open to the subpial space. Although the anatomical pathway that permits CSF from the basal cisterns to enter into leptomeningeal perivascular spaces has not yet been defined, it seems likely that fenestrations in the pia mater ensheathing vessels at the base of the brain allow CSF entry into the proximal perivascular network. CSF is then propelled rapidly through these perivascular spaces by arterial pulsations or by hydrostatic pressure gradients between different cisternal CSF compartments to enter the brain parenchyma along penetrating arteries.

Studies with fluorescent tracers demonstrate that CSF entering the brain along the Virchow–Robin space moves readily along the perivascular spaces surrounding the arteriolar wall, eventually reaching the basal lamina of cerebral capillaries [6]. This demonstrates that the Virchow–Robin space, the perivascular spaces, and the vascular basement membranes are connected and that CSF from cisternal compartments is rapidly transported along these pathways (Fig. 3.2D–G). Fluorescent CSF tracers <70 kD in size exchange quickly between perivascular spaces and the surrounding interstitium, whereas high-molecular-weight tracers (500–2000 kD) remain largely trapped within the perivascular spaces. This suggests that the 20–80 nm extracellular clefts between overlapping perivascular astrocytic end feet, which completely ensheath the cerebral vasculature, restrict the free movement of solutes and cells between perivascular spaces and the wider brain interstitium.

Role of Astrocytes

In addition to physically bounding perivascular spaces with end-foot processes, astrocytes also support both perivascular CSF influx and interstitial solute clearance through the activity of the astroglial water channel aquaporin-4 (AQP4). AQP4 is a trans-membrane water channel expressed in astrocytes throughout the brain and in ependymal cells lining the cerebral ventricles. In astrocytes, AQP4 is localized primarily to the perivascular end-foot process, with up to 50% of the end-foot surface facing the cerebral vasculature being occupied by square arrays of AQP4 (Fig. 3.3A–D) [1,2]. Perivascular CSF influx is dramatically reduced in *Aqp4*-null mice, as is the clearance of interstitial solutes [6]. A computational study provides a biophysical basis for the role of AQP4 in supporting perivascular bulk flow and the clearance of interstitial solutes [7]. In this model, water moves rapidly through the intracellular astrocytic network that bridges perivascular spaces surrounding cerebral arteries and veins. The ready exchange of water from the intracellular astrocytic network and extracellular water across the vast surface area of the nonperivascular

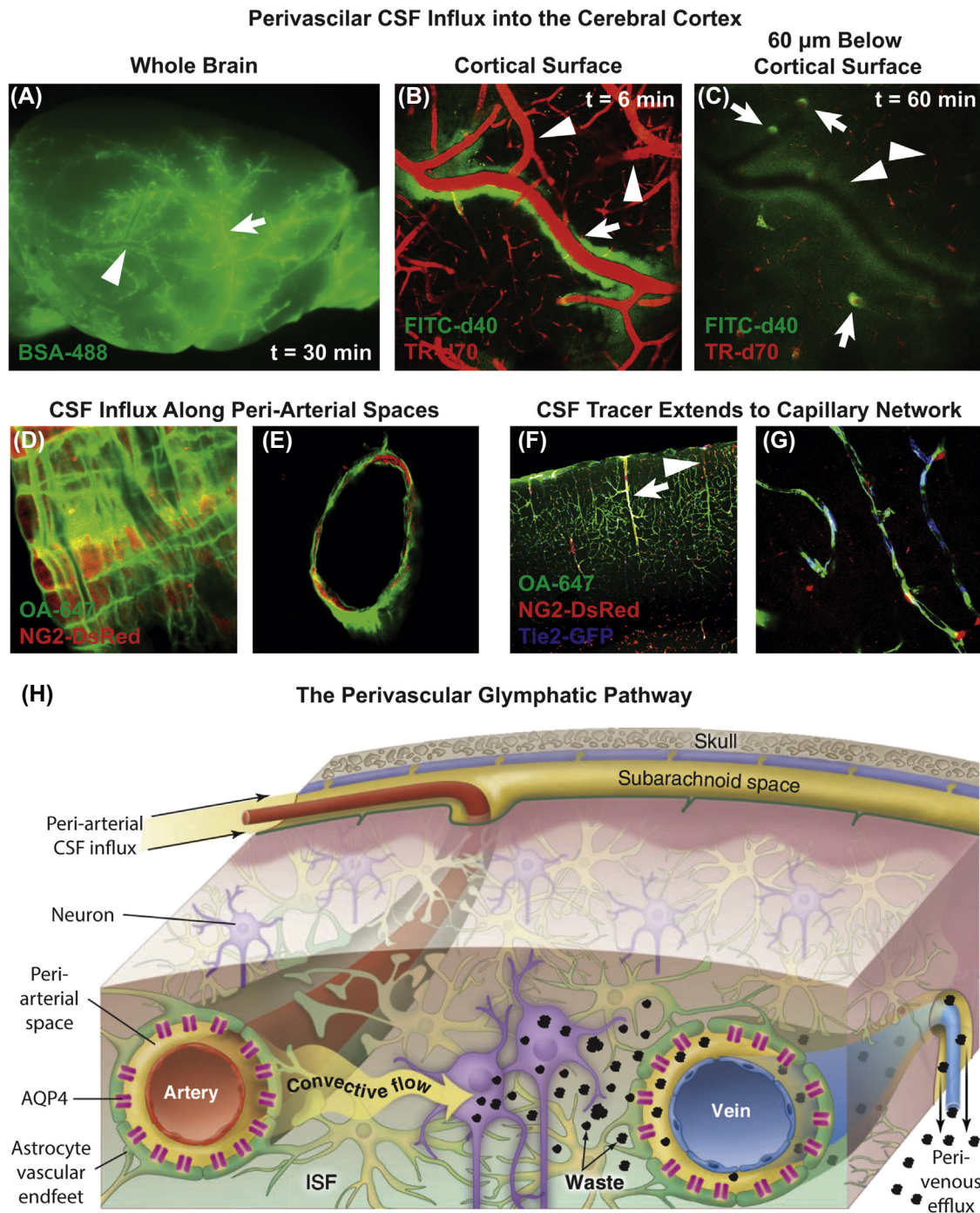


FIGURE 3.2 The glymphatic pathway supports the exchange of cerebrospinal fluid (CSF) and interstitial fluid (ISF) along perivascular pathways. CSF tracer moves through the subarachnoid space along perivascular pathways primarily surrounding cerebral surface arteries (arrows), but not veins (arrowheads) (A). (B, C) Dynamic two-photon imaging shows that CSF tracers enter the brain parenchyma within perivascular spaces along penetrating arterioles, then exchange with surrounding interstitial fluid. Confocal imaging shows that CSF tracer moves along basement membranes in the wall of penetrating arterioles (D, E), and reaches the basal lamina surrounding the cerebral microcirculation (F, G). (H) Schematic diagram showing overview of the perivascular glymphatic pathway. AQP4, aquaporin-4; BSA-488, bovine serum albumin-conjugated Alexa488 (65 kD, CSF tracer); FITC-d40, FITC-conjugated dextran (40 kD, CSF tracer); NG2-DsRed, red fluorescent protein driven under the NG2 promoter (vascular smooth muscle cell and pericyte marker); OA-647, ovalbumin-conjugated Alexa647 (45kD, CSF tracer); Tie2-GFP, green fluorescent protein driven under the Tie2 promoter (vascular endothelium marker); TR-d70, Texas Red-conjugated dextran (70kD, blood tracer). Reprinted from Illiff JJ, Wang M, Liao Y, et al. A paravascular pathway facilitates CSF flow through the brain parenchyma and the clearance of interstitial solutes, including amyloid beta. *Sci Transl Med* 2012;4(147):147ra111; Nedergaard *Science* 2013;340(6140):1529–30 with permission.

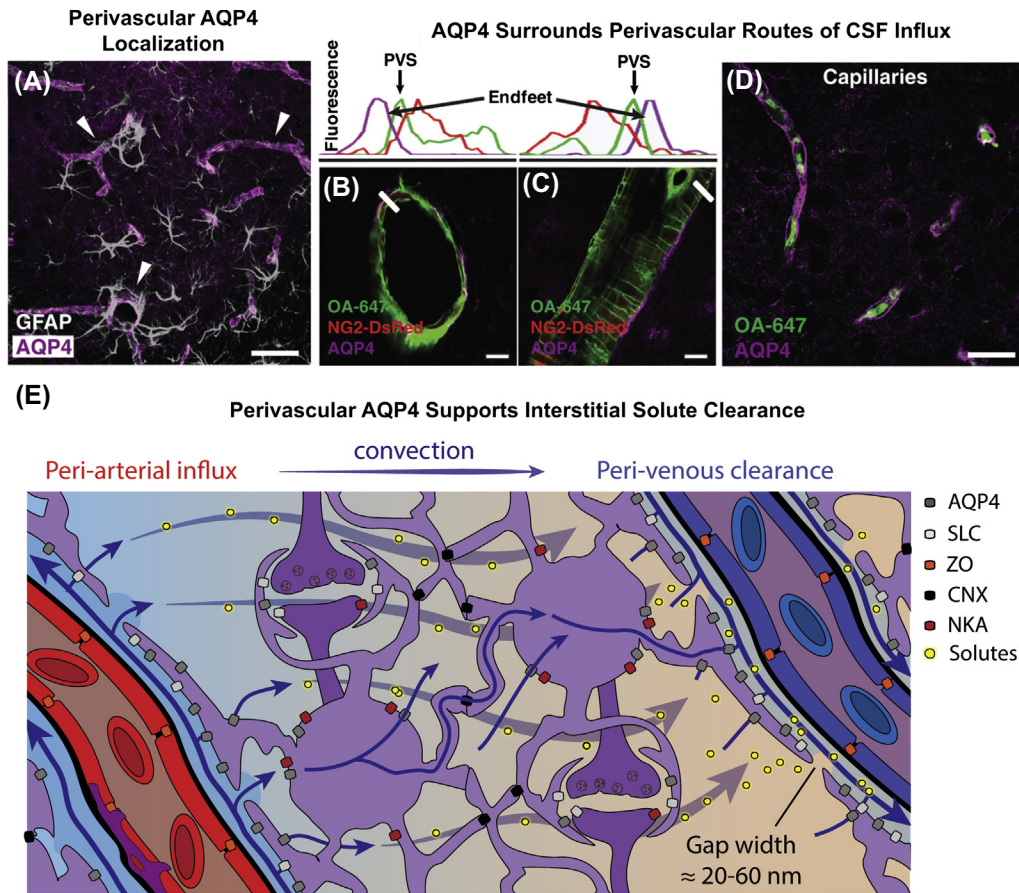


FIGURE 3.3 Localization of Aquaporin-4 (AQP4) to perivascular astroglial end feet supports interstitial solute clearance along the glymphatic pathways. (A) AQP4 is expressed in astrocytes and is localized primarily to perivascular astrocytic end feet surrounding the cerebral vasculature. (B, C) Perivascular cerebrospinal fluid (CSF) influx pathways are surrounded by AQP4-bearing perivascular end feet. (D) CSF follows perivascular spaces to reach terminal capillaries, which are surrounded by astroglial AQP4. (E) Schematic showing the role of astroglial water transport in supporting perivascular bulk flow and interstitial solute clearance. CNX, connexin; GFAP, glial fibrillary acidic protein; NG2-DsRed, red fluorescent protein driven under the NG2 promoter (vascular smooth muscle cell and pericyte marker); NKA, Na⁺-K⁺-ATPase; OA-647, ovalbumin-conjugated Alexa647 (45kD, CSF tracer); PVS, perivascular space; SLC, solute cotransporter proteins; ZO, zonula occludens. Reprinted and modified from Illiff JJ, Wang M, Liao Y, et al. A paravascular pathway facilitates CSF flow through the brain parenchyma and the clearance of interstitial solutes, including amyloid beta. *Sci Transl Med* 2012;4(147):147ra111; Thrane AS, Rangroo Thrane V, Nedergaard M. Drowning stars: reassessing the role of astrocytes in brain edema. *Trends Neurosci* 2014;37(11):620–628 with permission.

astroglial process helps to couple intracellular water flux to solute clearance through the interstitial compartment (Fig. 3.3E).

Sleep–Wake Regulation

Glymphatic pathway function including perivascular influx of CSF through and the clearance of interstitial solutes from the brain is a primary feature of the sleeping, rather than the waking, brain [5]. Compared with the naturally sleeping brain, the influx of fluorescent subarachnoid CSF tracers into the mouse cortex was reduced by more than 90% in the waking brain. The clearance of interstitial tracers was similarly reduced by a factor of two in the waking versus the naturally sleeping brain. Sleep–wake changes in the glymphatic pathway function appear to be underpinned by changes in extracellular volume, as

electrophysiological recordings demonstrated that a 65% increase in the extracellular volume fraction occurred between the sleeping and waking brain. Increasing the extracellular volume facilitates more rapid diffusion of interstitial solutes, supporting access to perivascular bulk flow pathways underlying efflux from the brain parenchyma. Similarly high glymphatic pathway function was observed under anesthesia with ketamine and xylazine, an anesthetic regimen associated with slow wave activity common to stage 3 and 4 non-rapid eye movement sleep. Sleep–wake changes in extracellular volume and glymphatic function appear to be regulated in part by cortical noradrenergic tone underlying arousal state, as local inhibition of cortical noradrenergic signaling with pharmacological antagonists increased the extracellular volume fraction and improved glymphatic pathway function in the waking state.

TERMINAL EFFLUX ROUTES

Perivascular pathways throughout the brain, including those surrounding large-caliber veins that drain into dural sinuses, facilitate the efficient clearance of interstitial solutes to the CSF. A fraction of subarachnoid CSF enters the brain along perivascular spaces surrounding penetrating cerebral arteries, indicating that some portion of the interstitial solutes recirculate through the brain parenchyma along the glymphatic pathway. The remaining CSF and its associated solutes are cleared from the cranium by bulk reabsorption with the CSF. Thus, the CSF compartment is a critical crossroad linking solute and fluid movement into and out of the brain interstitium with movement into and out of the blood stream. Although CSF reabsorption pathways are a topic covered in another chapter of this textbook and are not the central focus of the present chapter, it is important to articulate the functional connections between perivascular CSF-ISF exchange and the routes of terminal CSF efflux from the cranium, including the classically described arachnoid villi and perineural pathways, in addition to the recently described lymphatic vessels that are associated with dural sinuses and the dural vasculature.

Classical descriptions of CSF reabsorption focus on the role of arachnoid villi, valve-like structures within the walls of dural sinuses through which CSF enters the blood stream directly, as well as perineural sheathes, which surround cranial and spinal nerves and permit efflux of CSF and associated solutes to extracranial tissues and peripheral lymphatic vessels draining the head and neck [1,2]. The relative contribution of these classical CSF efflux pathways to the clearance of solutes originating within the brain interstitium is not clear at present, and may differ by species, and developmental and physiological state. One important distinction between these two pathways, however, is that transit via the arachnoid villi provides efflux directly to the blood stream, whereas reabsorption along perineural pathways involves clearance first along cranial lymphatic vessels to the deep cervical lymph nodes. This distinction may have important implications for the function of peripheral immune surveillance within the CNS and the surrounding CSF compartments.

The absence of conventional lymphatic vessels from the CNS has been a central feature of our understanding of BBB and CSF physiology for more than a century, dictating that the lymphatic functions of interstitial protein and fluid homeostasis and peripheral immune surveillance are accomplished within the brain in a manner distinct from that of other organs. However, a network of apparently classical lymphatic vessels associated with the dural sinuses and the dural vasculature were described in mice [8]. These vessels expressed

histological markers of lymphatic endothelial cells, were associated with a large number of peripheral T lymphocytes and antigen presenting cells, and provided an efflux pathway for tracers injected both into the CSF and the brain parenchyma to be drained to the cervical lymphatics via the deep cervical lymph nodes. Although these were termed a “cerebral lymphatic system,” it is notable that these lymphatic vessels do not appear to extend into brain tissue, but instead are associated with the outer layers of the meninges. For this reason, it appears likely that the perivascular glymphatic pathway, the CSF compartment, and the dural lymphatic vasculature are three elements of a single integrated system that supports the lymphatic functions of interstitial waste clearance and immune surveillance behind the curtain of the BBB and while maintaining the relative “immune privilege” of the CNS parenchyma.

PHYSIOLOGICAL ROLES OF PERIVASCULAR EXCHANGE AND CEREBRAL LYMPHATICS

In the periphery, the lymphatic vasculature makes important contributions to basic aspects of organ function, including ISF, lipid and protein homeostasis, and trafficking of lymphocytes and antigen presenting cells to lymph nodes. Within the brain, it appears that similar functions are supported by the combined activity of the perivascular glymphatic system, the CSF circulation, and sinus-associated lymphatic vessels [2,8].

Experimental studies defining the function of the glymphatic system and sinus-associated lymphatic vessels have focused on the clearance of relatively inert exogenous tracer molecules, including fluorescently or radiolabeled mannitol, inulin, dextrans, and polyethylene glycols, or proteins such as albumin or ovalbumin. Biologically active proteins such as amyloid β ($A\beta$) and tau, which are released into the brain extracellular space during neural activity, are also cleared along perivascular pathways [1,2]. Deletion of the *Aqp4* gene slows the clearance of soluble $A\beta$ by 55% [6], whereas $A\beta$ is cleared twice as quickly from the sleeping brain compared with the waking brain [5]. Sampling of mouse ISF by in vivo microdialysis and human CSF by serial lumbar CSF sampling demonstrates that levels of interstitial $A\beta$ increase during waking, and decline with sleep, whereas this drop in $A\beta$ during sleep is prevented by sleep deprivation [9]. These findings suggest that the clearance of potentially toxic metabolites, such as $A\beta$, from the brain interstitium by the glymphatic system may be one of the mechanisms underlying the restorative function of sleep.

A study describing the presence of classical lymphatic vessels associated with dural sinuses also reported that under quiescent conditions, T lymphocytes and antigen

presenting cells were strongly associated with these vessels [8]. Tracers injected both into the brain parenchyma and into the CSF drained through these lymphatic structures to the deep cervical lymph nodes, whereas ligation of the afferent drainage of the deep cervical lymph nodes caused the distension of sinus-associated lymphatic vessels and the accumulation of peripheral immune cells within the dura. These findings suggest that sinus-associated lymphatic vessels are a key site for peripheral immune surveillance of the CNS. Intriguingly, the choroid plexus is a key point of entry for peripheral immune cells into the CSF space. This suggests that drainage of interstitial solutes and antigens from the brain parenchyma along the perivascular glymphatic pathway to the CSF may permit interactions with immune cells originating in the choroid plexus, transiting the CSF compartments, and exiting along sinus-associated lymphatic vessels, permitting peripheral immune surveillance from the edge of the CNS, without compromising the relative immune privilege of the CNS.

PATHOLOGICAL ROLES OF PERIVASCULAR CEREBROSPINAL FLUID–INTERSTITIAL FLUID EXCHANGE

Cerebral Edema

Brain edema represents a potentially fatal buildup of excess fluid within the confines of the rigid skull. Edema can accumulate acutely, following, for instance, TBI or stroke, but it can also develop more chronically in the context of brain tumors or metastases. When excess edema fluid builds up predominantly inside cells as a consequence of impaired energy metabolism, it is normally referred to as cytotoxic edema. In the context of cerebrovascular disease, the traditional view is that cytotoxic edema results from net inward movement of water and salts across the BBB into ischemic and infarcted tissue. Vasogenic edema, on the other hand, usually develops days after a brain infarct, and is traditionally thought to involve a breakdown of the BBB, with consequent exudation of plasma proteins and extravasation of leukocytes. However, this traditional understanding of brain edema leaves several explanatory gaps. In the context of focal ischemia, brain edema principally accumulates in the better-perfused “penumbra,” rather than in the infarct core, where cellular metabolism is most severely affected. This ischemic penumbra becomes edematous within hours of arterial occlusion and before opening of the BBB in the setting of focal ischemia. Moreover, imaging studies indicate that brain edema is more prone to buildup in the interstitial rather than in the intracellular compartment, likely due to the robust volume regulation of astroglia *in vivo*. Finally, in the context of vasogenic

edema, salt and water exudation, rather than the osmotic effects of protein leakage, are best correlated with the degree of edema. It is therefore possible that redistribution of solutes into the infarct core would set up osmotic gradients that favor excess glymphatic influx of CSF into the still perfused penumbra. This acute influx of excess glymphatic fluid would depend on astroglial water-channel AQP4, consistent with previous experimental data on cytotoxic brain edema. A failure of the energy-deprived ischemic tissue to maintain ionic gradients and normal perivascular anatomy might also hinder glymphatic ISF clearance and contribute to the development of interstitial and cytotoxic edema (Fig. 3.4) [10]. In addition, during vasogenic edema one would expect the exudation of high-molecular-weight serum proteins and leukocytes to occlude perivascular pathways, creating “perivasculitis” that could further impair glymphatic ISF clearance and contribute to the edema. In summary, it therefore seems likely that glymphatic activity and brain edema are interconnected, but the exact details of how glymphatic pathway impairment might contribute to edema in the context of stroke and other brain pathologies remain to be determined.

Aging and Neurodegeneration

A hallmark of neurodegenerative diseases is the age-related accumulation of fibrillary protein aggregates, such as extracellular senile plaques comprising A β and intracellular neurofibrillary tangles comprising hyperphosphorylated tau in AD. Experimental studies carried out in rodents demonstrate that interstitial A β and tau are cleared from the brain interstitium during sleep along perivascular spaces surrounding large-caliber draining veins. In the aging rodent brain, glymphatic pathway function is impaired, including a slowing of perivascular CSF–ISF exchange and interstitial A β clearance [1,2]. In this setting, impaired glymphatic pathway function was closely associated with the loss of perivascular AQP4 localization, suggesting that mislocalization of astroglial AQP4 may be one of the features that renders the aging brain vulnerable to protein misaggregation and subsequent neurodegeneration. It is possible that similar mechanisms may underlie the aggregation of other proteins in other neurodegenerative conditions, such as α -synuclein in Parkinson disease or Lewy body dementia. Sleep disruption is also a common feature of aging [9], and may further contribute to the impairment of effective A β clearance along the glymphatic pathway. In two clinical studies focusing on subjects with mild cognitive impairment (before diagnosis with AD), worsening sleep quality or sleep duration were associated with A β plaque deposition evaluated either with CSF biomarker measurement or amyloid positron emission tomography imaging.

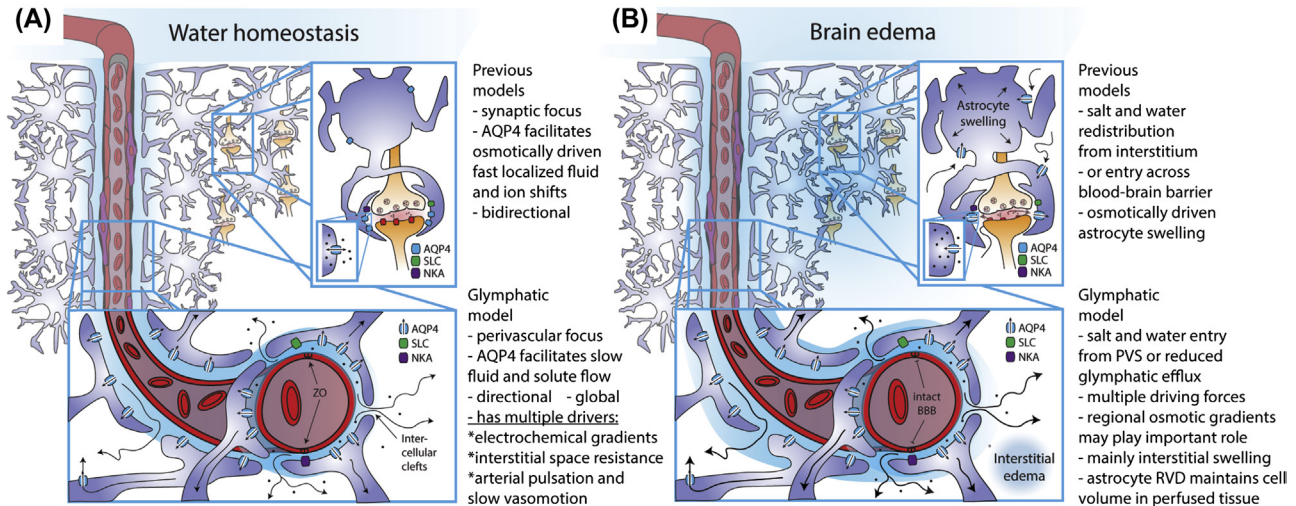


FIGURE 3.4 Proposed role of glymphatic pathway function in the development of cerebral edema after ischemic brain injury. Distinctions between previous models of salt and water homeostasis (*top*) and the glymphatic model (*bottom*) in the physiological setting (A) and in the setting of cerebral edema (B). In the glymphatic model, hydrostatic and electrochemical gradients drive fluid movement along perivascular spaces, whereas astroglial AQP4 supports fluid exchange along these pathways by permitting rapid water movement through the intracellular glial syncytium. In the setting of edema, perivascular salt and water entry combined with slowing glymphatic efflux results in interstitial swelling and inflammation within the perivascular space (“perivasculitis”). AQP4, aquaporin-4; NKA, Na⁺-K⁺-ATPase; OA-647, ovalbumin-conjugated Alexa647 (45 kD, CSF tracer); PVS, perivascular space; RVD, regulatory volume decrease; SLC, solute cotransporter proteins. Reprinted and modified from Thrane et al. *Trends Neurosci* 2015;38(6):333–5. <http://dx.doi.org/10.1016/j.tins.2015.04.009>. Epub 2015 May 22 with permission.

Chronic Glymphatic Pathway Impairment and Posttraumatic Neurodegeneration

TBI, including mild TBI (known commonly as concussion), is a risk factor for the development of early-onset dementia and AD. Among contact sport athletes and armed forces service members exposed to repeated mild TBI, a progressive tauopathy, chronic traumatic encephalopathy is characterized by perivascular deposits of tau aggregates initially in superficial layers of the cerebral cortex. The factors that make the posttraumatic brain vulnerable to neurodegeneration in the decades following injury are not clear. Experimental studies carried out in rodents demonstrate that after TBI, perivascular AQP4 localization and glymphatic pathway function is chronically impaired [1,2]. When glymphatic pathway function is impaired by *Aqp4* gene deletion, tau phosphorylation and neurocognitive deficits are worsened after moderate to severe TBI. This suggests that chronic impairment of glymphatic pathway function in the posttraumatic brain may set the stage for aberrant tau aggregation and neurodegeneration.

CONCLUSION

ISF and protein homeostasis and immune surveillance are two basic physiological functions that in the periphery are served by the lymphatic system. In the CNS, which is sheltered by the BBB, these vital functions must be accomplished through an alternative process. Emerging research suggests that in the brain these functions are

supported through the combined activity of the perivascular glymphatic pathway, the CSF circulation, and the recently described sinus-associated lymphatic vasculature. Because the physiological mechanisms underlying the cerebral glymphatic and dural lymphatic systems remain largely unexplored, we are only beginning to appreciate the role that their dysfunction may play in the development of neurovascular, neurodegenerative, and neuroinflammatory conditions. Although the studies that have defined glymphatic pathway function have focused primarily on the pathogenic events underlying the development of neurodegenerative diseases such as AD, it appears likely that the impairment of ISF clearance in the presence of ongoing perivascular CSF influx may be a key driver of the development of cerebral edema after stroke or TBI. Similarly, the development of perivasculitis, with BBB dysfunction and perivascular immune cell infiltration, may underlie many of the consequences of vasogenic edema associated with ischemic brain injury.

References

- [1] Jessen NA, Munk AS, Lundgaard I, Nedergaard M. The glymphatic system: a beginner’s guide. *Neurochem Res* 2015;40(12):2583–99.
- [2] Simon MJ, Iliff JJ. Regulation of cerebrospinal fluid (CSF) flow in neurodegenerative, neurovascular and neuroinflammatory disease. *Biochim Biophys Acta* 2015;1862(3):442–51.
- [3] Sykova E, Nicholson C. Diffusion in brain extracellular space. *Physiol Rev* 2008;88(4):1277–340.
- [4] Groothuis DR, Vavra MW, Schlageter KE, et al. Efflux of drugs and solutes from brain: the interactive roles of diffusional transcapillary transport, bulk flow and capillary transporters. *J Cereb Blood Flow Metab* 2007;27(1):43–56.

- [5] Xie L, Kang H, Xu Q, et al. Sleep drives metabolite clearance from the adult brain. *Science* 2013;342(6156):373–7.
- [6] Iliff JJ, Wang M, Liao Y, et al. A paravascular pathway facilitates CSF flow through the brain parenchyma and the clearance of interstitial solutes, including amyloid beta. *Sci Transl Med* 2012;4(147):147ra111.
- [7] Asgari M, de Zelicourt D, Kurtcuoglu V. How astrocyte networks may contribute to cerebral metabolite clearance. *Sci Rep* 2015;5:15024.
- [8] Iliff JJ, Goldman SA, Nedergaard M. Implications of the discovery of brain lymphatic pathways. *Lancet Neurol* 2015;14(10):977–9.
- [9] Lim MM, Gerstner JR, Holtzman DM. The sleep-wake cycle and Alzheimer's disease: what do we know? *Neurodegener Dis Manage* 2014;4(5):351–62.
- [10] Thrane AS, Rangroo Thrane V, Nedergaard M. Drowning stars: reassessing the role of astrocytes in brain edema. *Trends Neurosci* 2014;37(11):620–8.

CHAPTER

4

Cerebrospinal Fluid: Formation, Absorption, Markers, and Relationship to Blood–Brain Barrier

G.A. Rosenberg

The University of New Mexico, Albuquerque, NM, United States

INTRODUCTION

Cerebrospinal fluid (CSF) reflects pathology in the brain, and is essential in diagnosis of many neurological diseases, including those due to inflammation, infection, and immunological processes. CSF indicates pathological processes because of the continuity of the brain interstitial fluid (ISF) with the CSF across the ependymal lining of the ventricles. CSF and ISF are actively secreted by energy-requiring mechanisms: mainly epithelial cells make CSF in the choroid plexus, whereas capillaries and cellular metabolism form ISF. Both processes involve the sodium–potassium ATPase electrolyte pumps. ISF is thought to drain into the CSF spaces by movement along white matter tracts and perivascular spaces. When inflammatory cells cross the capillaries or are activated within brain, the brain edema that results causes brain swelling with raised intracranial pressure. CSF and ISF are continuously produced, resulting in about 500 mL per day, which must be removed or hydrocephalus will result. This dynamic system is routinely sampled for

diagnostic and therapeutic reasons, making it essential for the clinician to understand the underlying molecular physiology.

An important concept that was identified by early investigators was the limited capacity of the brain to swell due to the dura and the bones of the skull, which contain the brain tissue, blood, and CSF/ISF; increase in any of these compartments raises intracranial pressure, which if high enough can lead to herniation of the compressed tissue and death. The skull protects the vulnerable brain, composed of 80% water, from minor injury, but severe blows to the head result in movement of the brain tissues against the skull, creating damage to brain cells that can lead acutely to swelling with cell death and over longer periods to neurodegeneration.

Besides the strong external layers protecting vulnerable brain tissues, there are multiple, more delicate internal layers separating brain tissue from the systemic circulation and protecting the internal milieu from being exposed to blood cells and circulating proteins by

- [5] Xie L, Kang H, Xu Q, et al. Sleep drives metabolite clearance from the adult brain. *Science* 2013;342(6156):373–7.
- [6] Iliff JJ, Wang M, Liao Y, et al. A paravascular pathway facilitates CSF flow through the brain parenchyma and the clearance of interstitial solutes, including amyloid beta. *Sci Transl Med* 2012;4(147):147ra111.
- [7] Asgari M, de Zelicourt D, Kurtcuoglu V. How astrocyte networks may contribute to cerebral metabolite clearance. *Sci Rep* 2015;5:15024.
- [8] Iliff JJ, Goldman SA, Nedergaard M. Implications of the discovery of brain lymphatic pathways. *Lancet Neurol* 2015;14(10):977–9.
- [9] Lim MM, Gerstner JR, Holtzman DM. The sleep-wake cycle and Alzheimer's disease: what do we know? *Neurodegener Dis Manage* 2014;4(5):351–62.
- [10] Thrane AS, Rangroo Thrane V, Nedergaard M. Drowning stars: reassessing the role of astrocytes in brain edema. *Trends Neurosci* 2014;37(11):620–8.

 C H A P T E R

4

Cerebrospinal Fluid: Formation, Absorption, Markers, and Relationship to Blood–Brain Barrier

G.A. Rosenberg

The University of New Mexico, Albuquerque, NM, United States

INTRODUCTION

Cerebrospinal fluid (CSF) reflects pathology in the brain, and is essential in diagnosis of many neurological diseases, including those due to inflammation, infection, and immunological processes. CSF indicates pathological processes because of the continuity of the brain interstitial fluid (ISF) with the CSF across the ependymal lining of the ventricles. CSF and ISF are actively secreted by energy-requiring mechanisms: mainly epithelial cells make CSF in the choroid plexus, whereas capillaries and cellular metabolism form ISF. Both processes involve the sodium–potassium ATPase electrolyte pumps. ISF is thought to drain into the CSF spaces by movement along white matter tracts and perivascular spaces. When inflammatory cells cross the capillaries or are activated within brain, the brain edema that results causes brain swelling with raised intracranial pressure. CSF and ISF are continuously produced, resulting in about 500 mL per day, which must be removed or hydrocephalus will result. This dynamic system is routinely sampled for

diagnostic and therapeutic reasons, making it essential for the clinician to understand the underlying molecular physiology.

An important concept that was identified by early investigators was the limited capacity of the brain to swell due to the dura and the bones of the skull, which contain the brain tissue, blood, and CSF/ISF; increase in any of these compartments raises intracranial pressure, which if high enough can lead to herniation of the compressed tissue and death. The skull protects the vulnerable brain, composed of 80% water, from minor injury, but severe blows to the head result in movement of the brain tissues against the skull, creating damage to brain cells that can lead acutely to swelling with cell death and over longer periods to neurodegeneration.

Besides the strong external layers protecting vulnerable brain tissues, there are multiple, more delicate internal layers separating brain tissue from the systemic circulation and protecting the internal milieu from being exposed to blood cells and circulating proteins by

preventing the blood with toxic electrolyte and protein levels from mixing with the CSF/ISF. These multiple layers prevent cellular dysfunction by maintaining the stable internal milieu needed for normal brain cell function.

The first layer of protection is provided by the endothelial cells, which are joined together by tight junctions [1]. In addition to the physical barrier, there are molecular and enzymatic barriers, including carrier molecules that move substances in and out of the brain, delivering nutrients and removing toxins; enzymes in the endothelial cells degrade unwanted substances and prevent them from entering the brain. Another important interface between the blood and the CSF/ISF occurs at the choroid plexuses. Finally, another site of the blood–brain barrier BBB is the arachnoid villi cells in the subarachnoid space, which transfer CSF/ISF into the blood. All of the interfaces have a common property of being joined with tight junctions. The brain lacks a true lymphatic system to drain metabolic products and deliver nutrients. The CSF and ISF provide the lymphatic function, and have been referred to as the third circulation [2]. Thus this complex series of interfaces, acting as the brain’s lymphatic circulation, moves molecules between cells and along perivascular spaces.

Because of the unique interfaces formed at critical sites in the brain, immunological reactions are limited in brain tissue, creating a site of “immunological privilege” [3]. The tight junctions at each interface prevent the levels of electrolytes in the brain from fluctuating widely with changes in the systemic circulation, which would occur during strenuous exercise. The tight junctions prevent the entrance of large protein molecules into the brain, which results in 40 mg% of albumin in CSF normally with a corresponding level of 4 g in the blood. They also block entry of circulating blood cells.

Sampling of the CSF is a common clinical procedure that is relatively safe and inexpensive compared with other procedures, making it a cost-effective addition to the diagnostic workup. The aim of this chapter is to describe the physiology and biochemistry of the CSF and the blood–brain interfaces, particularly as they relate to stroke [4].

BLOOD–BRAIN INTERFACES

Elaborate protective mechanisms are found in the brain mainly to separate the blood from brain cells. Release of blood into the brain as occurs with the rupture of an aneurysm produces a devastating effect. Each of the sites where blood comes into contact with brain fluids has a specialized epithelial-like layer of cells. The major interface is formed by the endothelial

cells, which have specialized proteins between the cells that seal them together, forming tight junctions that prevent proteins and cells from passing, and maintains a high electrical resistance. In addition to the endothelial interface, there are similar tight junction proteins found at the choroid plexus and the arachnoid granulations (Table 4.1). Tight junctions are composed of membrane proteins, occludin, claudins, and junctional adhesion molecules. Other proteins that are important in the maintenance of the tight junction cytoplasmic scaffolding proteins include zonula occludens, actin cytoskeleton, and associated proteins, such as protein kinases, small GTPases, and heterotrimeric G-proteins.

Tight junctions restrict passage of all but lipid-soluble molecules. Albumin, for example, which is 4–5 g/dl in the blood, is normally less than 50 mg/dl in the CSF. An important function of the BBB is to maintain differences in the concentrations between the blood and the brain for many electrolytes (Table 4.2), and it prevents the wide fluctuations in blood levels of certain electrolytes related to food intake, exercise, and other factors.

TABLE 4.1 Three Interfaces Between Blood and Brain That Form the Sites of the Blood–Brain Barrier

Interface	Site	Anatomical Correlate
1. Blood–brain	Cerebral blood vessels	Tight junctions between endothelial cells; transport functions; basal lamina
2. Blood–cerebrospinal fluid (CSF)	Choroid plexuses	Tight junctions between epithelial cells lining the choroid plexus
3. CSF–blood	Arachnoid granulations and arachnoid layer of the meninges	Tight junctions between arachnoid cells; a one-way valve-like action of the arachnoid granulations

TABLE 4.2 Comparative Concentrations of Substances Between Cerebrospinal Fluid (CSF) and Blood

Substance	CSF Concentration	Blood Concentration
<i>ELECTROLYTES (MEQ/L)</i>		
Sodium	138	138
Potassium	2.8	4.5
Chloride	19	102
Bicarbonate	22	24
Calcium	2.1	4.8
<i>PROTEINS (MG/DL)</i>		
Total protein	35	7000
Albumin	16	3700
IgG	1.2	1000

BLOOD–CSF INTERFACE

Choroid plexuses are the major source of CSF. Epithelial cells line the apical surface of the choroid plexuses (Fig. 4.1). Choroid plexuses float freely in the lateral and fourth ventricles. The rate of production of CSF in animals and in man has been measured experimentally, by placing needles to infuse fluids into the lateral ventricles and draining needles into the cisterna magna. Using ventriculocisternal perfusion and the dye and isotope dilution methods, a substance is introduced into the perfusion solution, and the amount of its dilution can be used to calculate the rate of formation of new CSF. In man, the rate of CSF formation is about 0.3 mL/min or about 500 mL/day, which results in the turnover of the CSF several times during the day [5].

Sodium–potassium ATPase pumps on the outer surface of the epithelial cells provide the ionic imbalance that results in a chemiosmotic energy for CSF secretion with the water flowing along the osmotic gradient established by the removal of three sodium ions for two potassium ions returned to the cell. Carbonic anhydrase is also important in fluid formation, but the mechanism is uncertain. Osmotic agents, such as mannitol, reduce production of CSF. Inhibition of carbonic anhydrase by acetazolamide also reduces CSF production. The production of CSF

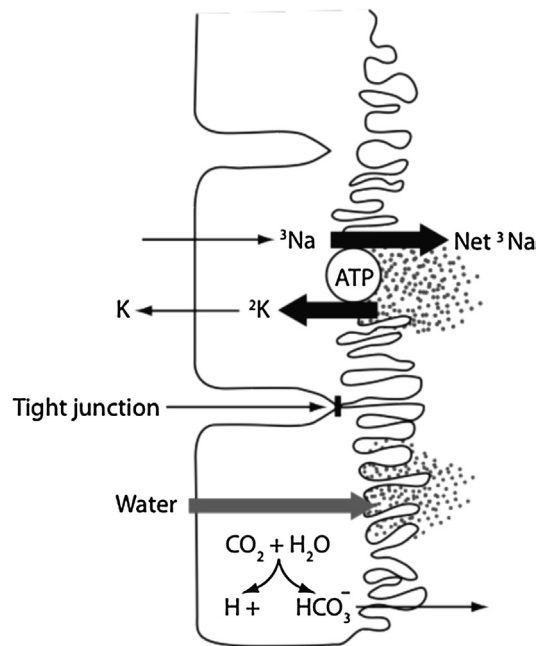


FIGURE 4.1 A schematic diagram of choroid plexus epithelial cells. Fenestrated capillary is shown in the stroma, which allows protein to escape. The epithelial cells have tight junctions between the apical surfaces, which also have the microvilli. An ATPase pump is on the apical surface. Carbonic anhydrase converts carbon dioxide to bicarbonate, which is removed into the cerebrospinal fluid and contributes protons to the sodium–proton exchange pump. Several other exchange pumps are shown.

is insensitive to increased pressure, and continues even when the CSF pressures are dangerously high.

Epithelial cells on the choroid plexus surface have tight junctions joining their apical surfaces. Beneath the epithelial cells is a stroma containing the blood vessels, which lack tight junctions. In this situation, there is no BBB but rather porous, fenestrated blood vessels in the stroma of the choroid plexus; tight junctions at the epithelial cell apical surfaces, providing the barrier at this interface, block larger molecules that leave the fenestrated blood vessels. The ependymal cells that form the surface of the choroid plexus are the site of the tight junctions, which is not the case in other ependymal covered regions that provide no barrier function, allowing fluid and proteins to pass from the CSF into the brain.

ISF production contributes to the CSF; estimates range from 30% to 60%, depending on the species. Most of the ISF formation is thought to be by the capillaries with a small contribution from metabolic water. In cats and rabbits, ISF is estimated to contribute 30% of the CSF, whereas in nonhuman primates some estimates are as high as 60% in an experiment where the choroid plexuses were removed [6]. Cerebral endothelial cells have an ATPase pump on the abluminal surface of the capillary, which is important in ISF formation. ISF moves through the 15–20% of brain that comprises the extracellular space and along perivascular pathways, combining with the CSF in the ventricles. Animal studies showed that substances injected into brain tissue appeared in the cervical lymphatics by draining along the olfactory nerves. The lymphatic route drains significant amounts of ISF in rats, cats, and rabbits, but the significance in humans is uncertain. Drainage of ISF into the cervical lymph nodes could allow brain antigens to enter the systemic circulation, causing an immunological response. The perivascular pathway conducts fluid transport within the brain. Astrocytes and capillaries are involved in the movement of fluid, and there appears to be a role for aquaporin, but the exact mechanism is uncertain [7]. Clearance of ISF via the perivascular route is altered in sleep [8]. The relevance of these studies done in mice to humans remains to be established.

The fluid formed by the cerebral blood vessels joins that formed by the choroid plexus in the cerebral ventricles, beginning the circulation of the CSF. From the ventricles the CSF exits into the cisterna magna through the foramina of Luschka and Magendie. Then, the CSF moves over the cerebral convexities. Arachnoid granulations absorb CSF into the blood. Cerebrospinal fluid percolates into the lumbar sac, where some is absorbed, before flowing up over the cerebral hemispheres.

Hydrocephalus results when the outflow of CSF from the cerebral ventricles is obstructed. This life-threatening situation requires surgical intervention to

insert a ventriculoperitoneal shunt. When the obstruction is at the level of the arachnoid granulations, resistance to absorption results in nonobstructed hydrocephalus. If the fluid is removed transependymally, normal pressure can occur. Selection of patients with normal pressure hydrocephalus for shunting is confounded in patients with white matter disease secondary to hypertension since the results of magnetic resonance imaging (MRI) can be confused in those two conditions [9].

CSF-BLOOD INTERFACE

Absorption of CSF occurs across the arachnoid villi by a valve-like mechanism. Electron microscopic images of the arachnoid granulations show a series of channel-like structures [10]. The channels behave as one-way valves, allowing CSF to drain into the blood, but preventing blood from entering the CSF. Absorption of the CSF is pressure dependent. The resistance to the outflow of CSF determines the CSF pressure. When the resistance to absorption is increased, the CSF pressure is raised. This occurs, for example, in bacterial meningitis or subarachnoid hemorrhage, where the white or red blood cells clog up the valve-like channels in the arachnoid granulations. Thus both the rate of CSF production and the resistance to CSF absorption contribute to the CSF pressure measured at a lumbar puncture.

CSF PRESSURE

CSF pressure can be measured during a lumbar puncture performed to collect CSF. Pressure measurements need to be done with the patient in the lateral recumbent position shortly after the needle is placed in the lumbar sac and, if possible, before fluid is removed; otherwise loss of fluid will interfere with an accurate measurement of pressure. When the patient is in a sitting position, the pressure cannot be measured.

Cerebral veins are the main contributors to the CSF pressure because the thin-walled veins transmit pressure from the vascular system to the CSF (Fig. 4.2A). Thicker-walled arteries with muscular layers exert less of an effect because the vessel walls create an equal and opposite force, preventing the transmission of pressure to the CSF. Venous pressure is lower than arterial, reflecting the pressure of the blood as it drains into the heart. Arteries contribute less to the CSF pressure than the veins. The correct location of the spinal needle in the thecal sac can be verified by observations of fluctuations in CSF pressure related to respiration; the expansion of the chest wall reduces the venous pressure and vice versa. The balance between production of CSF and absorption determines the CSF pressure; increased resistance to absorption results in an increase in CSF pressure (Fig. 4.2B).

Diseases that can cause an increase in venous pressure in the heart can lead to increased intracranial pressure, headaches, and rarely papilledema. Increases in

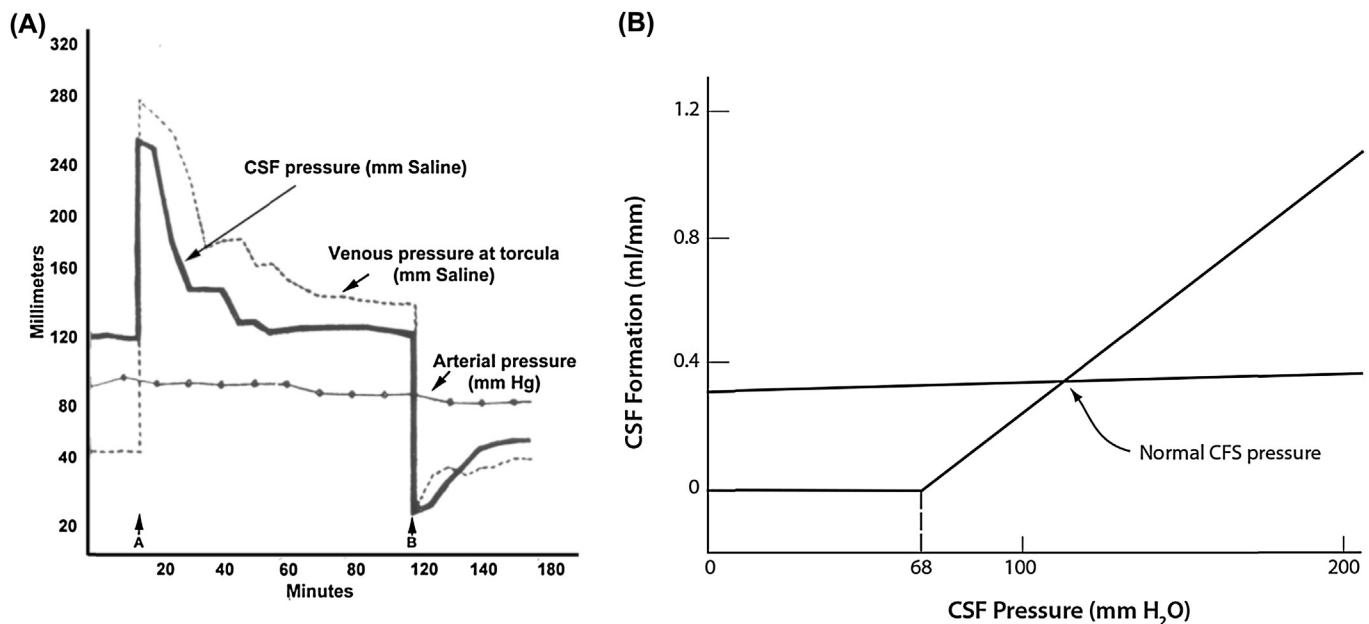


FIGURE 4.2 (A) Graph of influence of arterial and venous pressures on measurement of cerebrospinal fluid (CSF) pressure. Increase in CSF pressure is shown to be driven by the venous pressure, whereas there is no influence from arterial pressure. (B) Absorption of CSF is shown to begin at a CSF pressure of 68 mm H₂O, and to gradually increase as a function of absorption at the arachnoid villi. Formation of CSF is shown as a constant. The CSF pressure is a function of the rates of absorption and formation (arrow). Composite drawing modified from Rosenberg GA. *Molecular physiology and metabolism of the nervous system*. New York, USA: Oxford University Press; 2012.

arterial blood pressure affect CSF pressure only when drastic changes in blood pressure occur. For example, malignant hypertension in eclampsia dilates cerebral capillaries, leading to brain edema and increased CSF pressure. Benign intracranial hypertension is a poorly understood syndrome where the CSF pressure is markedly elevated.

There are a number of causes of increased intracranial pressure. Failure to absorb CSF can lead to hydrocephalus, which in the elderly can have normal pressure probably due to the opening of other absorption routes such as the transependymal absorption. In young obese women an idiopathic increase in intracranial pressure can occur [11]. In addition to unknown causes it can be due to medications, such as vitamin A and antibiotics, and to occlusion of the venous sinuses draining blood from the brain. Increased intracranial pressure can produce sixth nerve palsies as a remote effect because of the long course of the sixth nerve and the sharp bend over the clivus. Headache is the most common symptom, and many patients have visual obscurations. Papilledema is the major finding; the vision is preserved until the swollen optic disc encroaches on the macula. It is possible to follow the severity of the papilledema by serial measurements of the size of the blind spot created by the optic disc. Treatment with acetazolamide or steroids is helpful. Occasionally patients need a lumboperitoneal shunt to drain excess fluid. When vision is threatened, the optic nerve sheath fenestration can be done surgically. When the venous sinuses are blocked, there is some evidence that placement of a stent to open the sinus can be

helpful [12]. However, there are no controlled trials to assess this approach, and some of the improvement may have occurred spontaneously.

BLOOD–BRAIN BARRIER INTERFACE

The large surface areas of the cerebral capillaries make the BBB the most important of the interfaces between the blood and brain tissue (Fig. 4.3). Cerebral capillaries are unique and differ from systemic capillaries (Table 4.3). They have endothelial cells with continuous tight junctions. Sodium–potassium ATPase pumps are found on the abluminal side of the vessel. Glucose and amino acids undergo carrier-mediated transport. Enzymes are present in the vessel that degrade substances and prevent them from crossing the capillary. An extracellular matrix forms a basal lamina around the capillaries and arterioles (Fig. 4.4).

Brain tissue requires a constant supply of glucose and amino acids for normal metabolism. Cerebral capillaries have glucose transporter molecules that participate in the carrier-mediated transport across the capillary [13]. Abnormalities in the glucose transporter lead to reduced brain glucose and cellular damage. Monoamine oxidase, both A and B types, deaminate and inactivate biogenic amines, preventing them from entering the brain. Other enzymes identified in brain capillaries include choline acetyltransferase, which is important in choline metabolism, and γ -glutamyl transpeptidase, which is used as a marker for blood vessels.

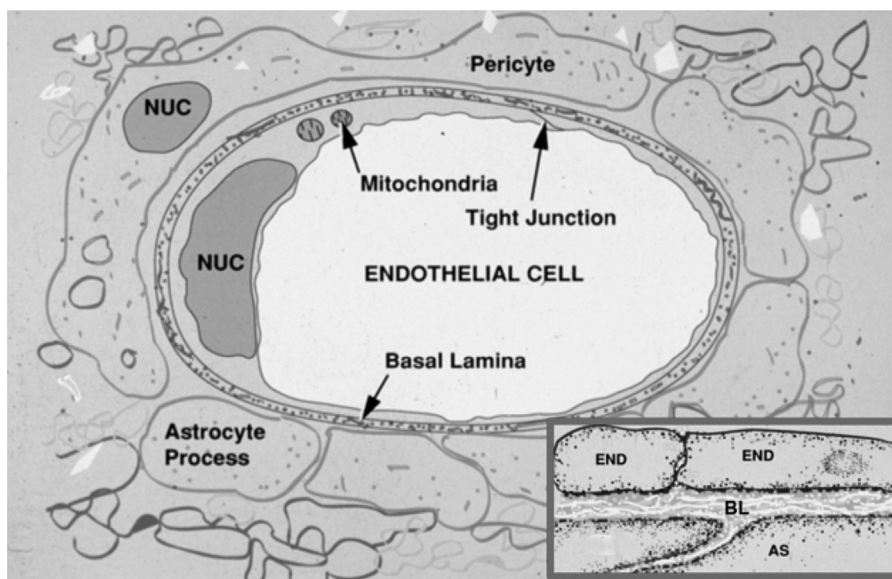


FIGURE 4.3 Drawing of cerebral capillary derived from an electron micrograph. The tight junctions are shown. Increased numbers of mitochondria are shown. Pericytes and astrocytes are shown around the blood vessels. Insert: Basal lamina of cerebral capillary is shown in this electron micrograph tracing. Endothelial cells are separated by basal lamina from astrocytes and pericytes. AS, astrocyte; BL, basal lamina; END, endothelial cell; NUC, nucleus.

TABLE 4.3 Unique Features of Cerebral Capillaries Important in the Blood–Brain Barrier

1. Tight junctions (zonula occludens)
2. Sodium–potassium ATPase
3. Carriers for glucose and amino acids
4. Proteolytic enzymes
5. Basal lamina

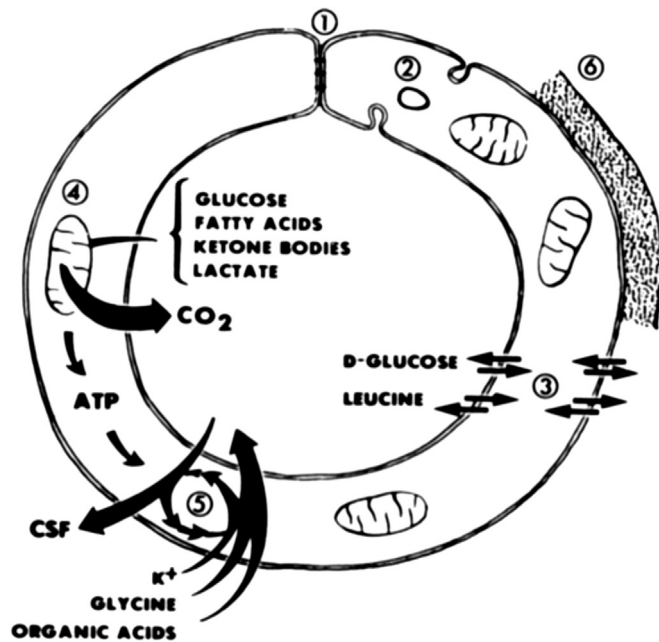


FIGURE 4.4 Cerebral capillary with its main functions. (1) Tight junctions, (2) few pinocytotic vesicles, (3) transport of glucose and amino acids, (4) large number of mitochondria, (5) secretion of cerebrospinal fluid by ATP-dependent pumping, and (6) basal lamina [4].

The glucose transporter is found in higher concentration in the cerebral capillaries than in most systemic vessels. At low blood glucose concentrations the carrier is unsaturated and helps movement of glucose into the brain along with diffusion. At high serum glucose concentrations the carrier molecule becomes saturated, and any additional transport is by diffusion alone. Specific carrier molecules in the cerebral blood vessel also transport amino acids into the brain. Competitive inhibition of a carrier causes reduced transport of essential substances. For example, an amino acid carrier transports L-Dopa, which is used to treat Parkinson disease, into brain. When a large protein meal is digested, other amino acids compete for the carrier sites, and less of the drug is absorbed. Another example is found in patients with an enzyme deficiency that leads to accumulation of excessive amounts of phenylalanine in the blood. Phenylalanine competes with the essential amino acid, tryptophan, reducing its absorption into the brain. Reduction of levels of phenylalanine in the blood

through dietary restrictions can prevent permanent brain damage.

Basal lamina surrounds the capillary. It is composed mainly of type IV collagen and laminin along with lesser amounts of fibronectin and heparan sulfate. The function of the basal lamina in brain is uncertain. In other organs it plays an important physiological role in control of permeability. For example, type IV collagen provides a layer of structural support around the blood vessel, heparan sulfate is a charge barrier, and laminin and fibronectin bind hormones and growth factors.

Proteolytic enzymes participate in the modulation of BBB permeability. These enzymes are important in injury and repair, complicating attempts to block their actions with drugs. The major proteases involved in the BBB are the matrix-degrading metalloproteinases, which are neutral proteases that break down the extracellular matrix in many pathological processes, including those involving brain, but they are also important in angiogenesis and neurogenesis during tissue repair after injury. Several brain cells make matrix metalloproteinases and other proteases in response to injury [14].

Several types of molecules can cross the BBB. Lipids dissolve in the membrane and equilibrate rapidly in brain with levels in the blood. Substances that are not lipid soluble enter the brain more slowly. The ability of a substance to cross the cerebral capillary determines its therapeutic potential. For example, heroin is a chemically modified morphine molecule that more rapidly enters the brain. Penicillin slowly crosses the BBB, whereas the newer generations of antibiotics, such as cephalosporin, more easily enter the brain. Drugs used to treat cancer, such as methotrexate, only slowly enter the brain. Injection into the thecal sac can be used to increase the amount of the agent reaching brain tissue. Increasing the ability of a drug to cross the BBB is a major area of research especially for drug companies.

PATHOLOGICAL CHANGES IN THE CAPILLARY

Cells can survive many insults if the cell's membranes remain intact. During an injury, when membranes break down the cells die. Less dramatic forms of cell death occur with the orderly involution of a cell during apoptosis and with autophagy [15]. Another consequence of damage to the cell is brain edema: when the cells swell and the membrane is intact, there is cytotoxic edema; damage to the blood vessels results in vasogenic edema. Capillaries affected by the injury have increased permeability, which results in the movement of solutes and water into the brain. Brain cells do not necessarily die of brain edema alone. Vasogenic edema spreads through

white matter in the extracellular space. Either cytotoxic or vasogenic edema can contribute to the tissue damage and interfere with recovery.

Opening of the BBB can be determined radiologically by computed tomography (CT) or MRI, using the injection of an appropriate contrast agent into the blood. Contrast-enhanced CT and MRI show leakage of a contrast agent into the brain in tumors, inflammation, and injury. For example, serial MRI in patients with multiple sclerosis has shown that the blood vessel is damaged before the formation of permanent changes in the myelin and blood vessel inflammation contributes to the demyelinating process [16].

Bacterial meningitis causes opening of the BBB in and around the subarachnoid space. The blood vessels in the subarachnoid space penetrate into the cortex along the Virchow–Robin spaces. As the vessels enter the cortex they have glial limitans around them, but deeper in the cortex, they have the basal lamina. Inflammatory cells derived from the meningeal vessels can enter the Virchow–Robin spaces and cause inflammation of the cortical surface. Antibiotics cause the bacterial cell walls to lyse with the release of toxic bacterial cell wall products, including lipopolysaccharide. Cytokines are formed, along with free radicals and proteases, which result in secondary damage to the blood vessel. Thus the antibiotic can control the infection, but the secondary damage can produce delayed vasogenic edema. In childhood meningitis treatment, steroids are given along with antibiotics to reduce the secondary damage from the inflammatory response, but use of steroids has not been adequately tested in adults with meningitis.

Cerebral ischemia causes opening of the BBB. The factors involved in the opening of the BBB are complex and include cytokines, free radicals, and proteases. Permanent occlusion of a blood vessel damages the cerebral capillaries in the ischemic tissue. Animal studies have shown that when the tissue undergoes reperfusion, BBB injury occurs more rapidly and is more severe. Reintroduction of oxygenated blood into the damaged tissue allows free radicals to form and neutrophils to enter the tissue, worsening the ischemic damage. The critical factor is to reduce the time before reperfusion to reduce the subsequent reperfusion injury.

CONCLUSION

The interfaces between blood and brain preserve the integrity of the neuronal microenvironment. Choroid plexuses and cerebral capillaries form CSF and ISF, which circulate through the cerebral ventricles and the extracellular spaces, leaving the brain mainly via the arachnoid granulations. CSF functions as the brain's lymph,

delivering nutrients and removing metabolic products. At each interface between blood and brain, anatomic or enzymatic processes are present that block movement of substances that are not lipid soluble. Carrier-mediated processes transport nutrients essential to brain cell function, such as glucose and amino acids, into the central nervous system. The BBB is frequently opened during injury, allowing brain edema to form, causing damage to brain cells. Many cytotoxic factors, including free radicals, cytokines, and proteases, participate in disruption of the BBB. Understanding the interaction of multiple factors in these processes will lead to more effective therapeutic agents.

References

- [1] Hawkins BT, Davis TP. The blood–brain barrier/neurovascular unit in health and disease. *Pharmacol Rev* 2005;57(2):173–85.
- [2] Cushing H. *The third circulation*. London: Oxford University Press; 1925.
- [3] Yong VW, Rivest S. Taking advantage of the systemic immune system to cure brain diseases. *Neuron* 2009;64(1):55–60.
- [4] Rosenberg GA. *Molecular physiology and metabolism of the nervous system*. New York, USA: Oxford University Press; 2012.
- [5] Cserr HF. Physiology of the choroid plexus. *Physiol Rev* 1971;51:273–311.
- [6] Milhorat TH, Hammock MK, Fenstermacher JD, et al. Cerebrospinal fluid production by the choroid plexus and brain. *Science* 1971;173:330–2.
- [7] Iliff JJ, Wang M, Zeppenfeld DM, et al. Cerebral arterial pulsation drives paravascular CSF–interstitial fluid exchange in the murine brain. *J Neurosci* 2013;33(46):18190–9.
- [8] Xie L, Kang H, Xu Q, et al. Sleep drives metabolite clearance from the adult brain. *Science* 2013;342(6156):373–7.
- [9] Brean A, Fredo HL, Sollid S, et al. Five-year incidence of surgery for idiopathic normal pressure hydrocephalus in Norway. *Acta Neurol Scand* 2009;120(5):314–6.
- [10] Upton ML, Weller RO. The morphology of cerebrospinal fluid drainage pathways in human arachnoid granulations. *J Neurosurg* 1985;63:867–75.
- [11] Bastin ME, Sinha S, Farrall AJ, et al. Diffuse brain oedema in idiopathic intracranial hypertension: a quantitative magnetic resonance imaging study. *J Neurol Neurosurg Psychiatry* 2003;74(12):1693–6.
- [12] Higgins JN, Cousins C,owler BK, et al. Idiopathic intracranial hypertension: 12 cases treated by venous sinus stenting. *J Neurol Neurosurg Psychiatry* 2003;74(12):1662–6.
- [13] Spector R. Nutrient transport systems in brain: 40 years of progress. *J Neurochem* 2009;111(2):315–20. doi:JNC6326 10.1111/j.1471-4159.2009.06326.x, [Published Online First: Epub Date] [pii].
- [14] Candelario-Jalil E, Yang Y, Rosenberg GA. Diverse roles of matrix metalloproteinases and tissue inhibitors of metalloproteinases in neuroinflammation and cerebral ischemia. *Neuroscience* 2009;158(3):983–94. S0306-4522(08)00895-6 10.1016/j.neuroscience.2008.06.025, [Published Online First: Epub Date] [pii].
- [15] Iadecola C, Anrather J. The immunology of stroke: from mechanisms to translation. *Nat Med* 2011;17(7):796–808. <http://dx.doi.org/10.1038/nm.2399>. [Published Online First: Epub Date].
- [16] Filippi M, Rocca MA, Barkhof F, et al. Association between pathological and MRI findings in multiple sclerosis. *Lancet Neurol* 2012;11(4):349–60. [http://dx.doi.org/10.1016/S1474-4422\(12\)70003-0](http://dx.doi.org/10.1016/S1474-4422(12)70003-0). [Published Online First: Epub Date].

CHAPTER

5

Anatomy of Cerebral Veins and Dural Sinuses

E. Egemen¹, I. Solaroglu²¹Koç University Hospital, Istanbul, Turkey; ²Koç University, Istanbul, Turkey

INTRODUCTION

Venous infarction of brain comprises only 1% of all strokes [1]. Many predisposing conditions such as dehydration, coagulopathies, pregnancy, trauma, surgical interventions, inherited collagen disorders, and autoimmune vascular diseases may result in cerebral vein thrombosis. Fortunately not all of veins lead to severe complications. However, in case of clinical manifestations developed, diagnosis must be done immediately in order to investigate and treat possible reasons. This chapter aims to present anatomical configuration of cerebral venous system regarding possible significant origin of “stroke.”

DURAL VENOUS SINUSES

The dural sinuses are large endothelial-lined trabeculated channels that collect cerebral blood from the superficial, deep, and posterior fossa and drain into the internal jugular vein at the level of the jugular bulb (Fig. 5.1) [2]. These sinuses, which lie between the superficial (periosteal) and deep (meningeal) layers of the dura mater, also excrete cerebrospinal fluid (CSF) via arachnoid granulations (i.e., Pacchionian granulations) that emerge from the subarachnoid space [3]. These arachnoid granulations (villi) are commonly found around the superior sagittal and transverse sinuses [1]. Furthermore, cavernous sinuses (CS), which are paired dural venous sinuses, contain cranial nerves, arteries, and veins.

Superior Sagittal Sinus

The superior sagittal sinus (SSS), which is the longest dural sinus, lies along the superior edge of the falx cerebri, which is attached to the crista galli at the

interhemispheric space just underneath the cranial vault. The SSS originates from the anterior part of the frontal lobe at the foramen caecum and drains into the torcular herophili [4]. Contact with the SSS leads to the development of an impression on the frontal and parietal bone.

The SSS enlarges posteriorly due to tributaries from cortical veins and arachnoid granulations. Concurrently, emissary veins carry diploic blood into the SSS. Thus, the posterior portion of the SSS is more visible in the venous phase of digital subtraction angiography (DSA) and magnetic resonance venography (MRV). The radiological appearance of the SSS is curvilinear with an enlarged line in the sagittal view and a reverse triangular shape in the coronal view. A rudimentary view of the anterior one-third portion of the SSS has been well characterized [5].

Inferior Sagittal Sinus

The inferior sagittal sinus (ISS) originates from the inferior edge of the anterior one-third portion of the falx cerebri and lies within the interhemispheric spaces. This relatively small sinus collects anterior pericallosal veins [3]. The ISS has a curvilinear shape like the SSS. The ISS joins with the great cerebral vein (i.e., vein of Galen) at the level of the falcotentorial junction, which both drain into the straight sinus [5].

Straight Sinus

The straight sinus (SS) originates from the falcotentorial junction via the union of the great cerebral vein and the ISS. The SS receives veins from the falx cerebri, tentorium cerebelli, and adjacent brain parenchyma. The SS drains into the torcular herophili together with the SSS [3]. As a variation, the SS may also drain into the transverse sinus; this variation tends to occur more frequently on the left side [1].

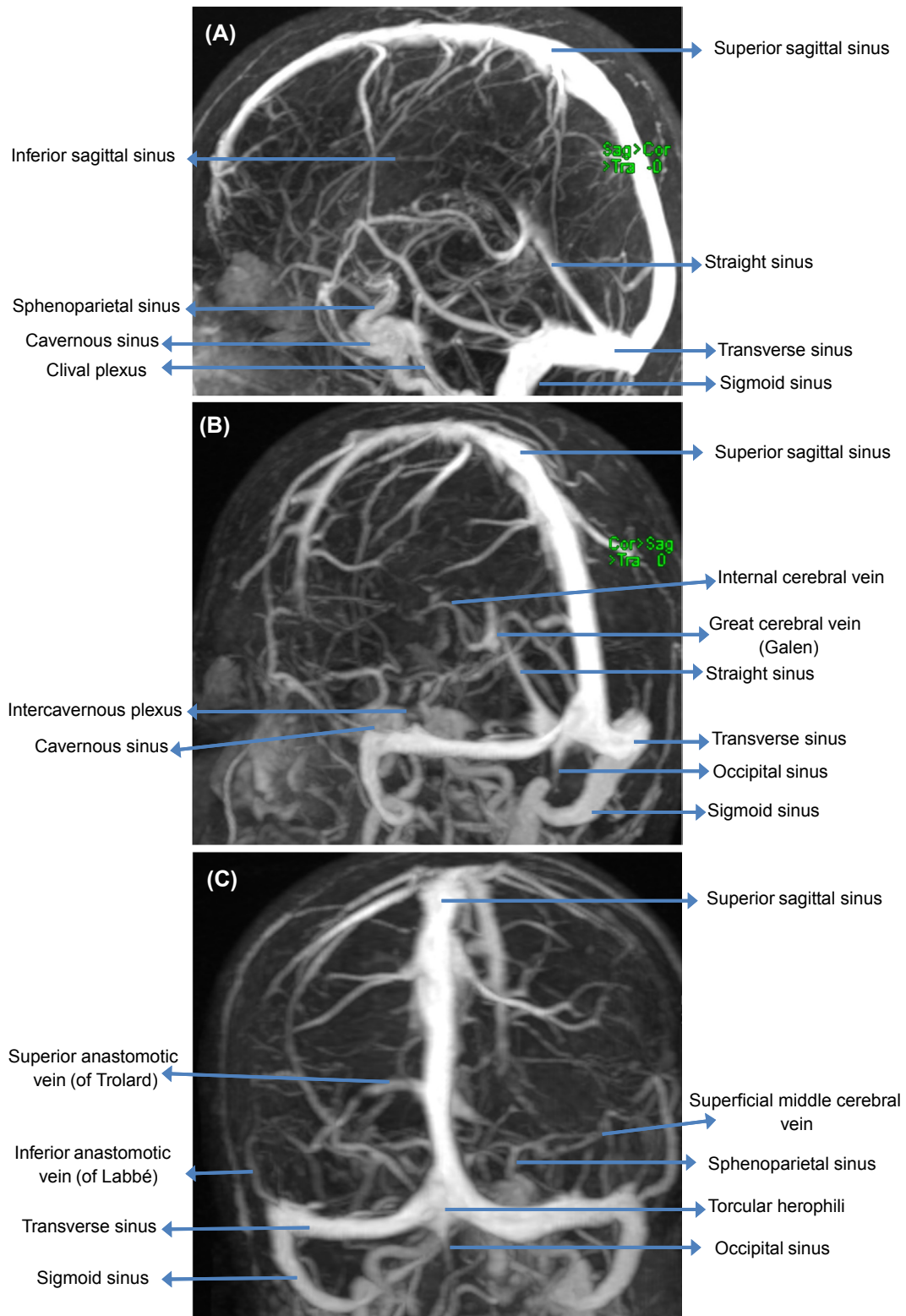


FIGURE 5.1 Magnetic resonance venography of brain with lateral (A), oblique (B), and anteroposterior (C) views. Superior sagittal, straight, and occipital sinuses join at the point of torcular herophili. Then they drain into transverse, sigmoid sinuses and internal jugular vein orderly. Superficial middle cerebral vein makes anastomosis to superior sagittal sinus via vein of Trolard, to transverse sinus via vein of Labbé, and to cavernous sinus via sphenoparietal sinus. Intercavernous plexus and clival plexus also make connection between two cavernous sinuses.

Transverse (Lateral) Sinuses

The transverse (lateral) sinuses (TS) originate from the torcular herophili and drain into the sigmoid sinuses. The TS are located at the posterior edge of the tentorium cerebelli. Like the SSS, the TS also absorb CSF via arachnoid granulations. The TS are mostly asymmetric; the right TS tends to be larger [3]. Radiological view of hypoplastic TS or absence of TS should differentiate from TS thrombosis.

Torcular Herophili (Confluens Sinuum)

The torcular herophili, which are also known as the confluence of sinuses (confluens sinuum), represents the crossroads of the SSS, ISS, TS, and the occipital sinus, when present [3]. Anatomical localization of the torcular herophili is varied. The torcular herophili appear as an asymmetric pouch in the radiological view [5].

Sigmoid Sinuses

Sigmoid sinuses are so named due to their S-shaped curves extending from the lateral edge of the tentorium cerebelli to the jugular bulb. Asymmetry can be seen in accordance with asymmetry in TS [3].

Cavernous Sinuses

These complex large sinuses are about 2 cm long and 1 cm wide including trabeculations and contain important vessels and cranial nerves. Anatomically placed laterally to the sella turcica both CS are connected by intercavernous venous plexus at anterior and posterior edge of sella turcica and also by clival venous plexus [6].

The main tributaries of the CS are the superior and inferior ophthalmic veins and the sphenoparietal sinuses. Thus, the CS collect blood from not only the inferior parts of the frontal and parietal lobe but also the orbital cavity [4]. Sphenoparietal sinuses are anastomotic vein, which are placed on lesser sphenoid wing and make connection between CS and superficial middle cerebral vein (Sylvian vein) and also receive veins of temporal pole. The CS also receive tributaries from the skull base via the superior and inferior petrosal sinuses [3].

Cavernous segment of internal carotid artery enters in CS and runs posteriorly to superior (posterior ascending segment), then turns anteriorly in middle part of CS (horizontal segment) and before exit from CS runs to superior (anterior ascending segment) [6].

Oculomotor nerve (CNIII), trochlear nerve (CNIV), and ophthalmic divisions of trigeminal nerve (CNVI) attach to lateral wall of CS and leave intracranial space

via superior orbital fissure. Maxillary divisions of trigeminal nerve (CNV2) also attach to the lateral wall of CS, however, exit extracranial space via foramen rotundum. Abducens nerve (CNVI) is in middle part of CS, which is placed laterally to the ICA [6].

Superior and Inferior Petrosal Sinuses

The superior petrosal sinuses (SPS) are located between the petrous part of the temporal bone and anterolateral edge of the tentorium cerebelli. The SPS connect the CS to sigmoid sinuses and less frequently to TS. The inferior petrosal sinuses (IPS) lie on the petro-occipital fissure and drain the CS into the jugular bulb via the clival venous plexus [3].

Occipital Sinus

The occipital sinus, which is the smallest dural venous sinus, runs along the inner surface of the occipital bone. The occipital sinus is attached to the posterior margin of the falx cerebelli and receives tributaries from the margins of the foramen magnum. It may anastomosis with the sigmoid sinuses and posterior internal vertebral plexus that drain into the torcular herophili. The occipital sinus is an important vascular structure during posterior fossa surgery. Variations in the occipital sinus, such as double or oblique occipital sinuses or the absence of the occipital sinus, are observed in rare cases [7].

CEREBRAL VEINS

Cerebral veins accompany arteries in the subarachnoid space. Unlike veins in other parts of the body, cerebral veins do not have valves. Thus, bidirectional flow is possible in cerebral veins. The walls of cerebral veins are thin and vulnerable as they do not contain muscle tissue. Cerebral veins are subdivided into three groups according to their anatomical location [2]:

1. superficial venous system (external);
2. deep venous system (internal);
3. veins of the brain stem and posterior fossa.

Superficial Supratentorial Cortical Veins (External)

Superficial supratentorial cortical veins are located on the surface of the brain and categorized into three main groups according to their drainage [3].

- *Superior Cortical Veins*: These veins are also known as the superior sagittal group because they drain into the SSS [1]. The most prominent vein of this group is the superior anastomotic vein, which is

known as the vein of Trolard. This anastomotic vein connects the superficial middle cerebral vein (SMCV) to the SSS. In addition, there are 8–12 unnamed smaller veins in the upper part of the hemispheric convexity [2].

- *Middle Cortical Veins:* These veins are also known as the sphenoidal group because they drain into the CS via the sphenoparietal sinuses. The dominant vein in this group is the SMCV, which is also known as the Sylvian vein due to its location in the Sylvian fissure (i.e., the lateral cerebral fissure). Middle cortical veins receive tributaries from the inferior part of the frontal lobe, superior temporal gyrus, and parietal opercula. The vein of Labbé (Fig. 5.2), which is another anastomotic vein of the SMCV, receives tributaries from the posterior and inferior temporal lobe and adjacent parietal lobe and drains primarily into the TS and rarely into the sigmoid sinuses [2].
- *Inferior Cortical Veins:* The major vein of this group is the deep middle cerebral vein (DMCV), which receives tributaries from the inferior frontal lobes and temporal lobes such as the insula, basal ganglia, and parahippocampal gyrus. The basal vein of Rosenthal (BVR), which is considered part of the deep venous system, is an anastomotic vein of the DMCV [2,3].

Deep Supratentorial Cortical Veins (Internal)

Deep structures of the cerebral hemispheres, including the basal ganglia, corpus callosum, thalamus, and posterior part of the limbic system, are drained by the deep venous system, which has two major components: internal cerebral vein (ICV) and BVR [1].

Numerous smaller medullary veins emerge from the subcortical area, directly cross the white matter, and drain into the subependymal veins. Septal veins and thalamostriate veins are the most prominent vascular structures of subependymal veins. Septal veins are localized to the frontal horn and course posteriorly toward the septum pellucidum. Thalamostriate veins are anatomically located medially to the caudate nucleus and thalamus [3]. These two veins meet near the foramen of Monro which is composed of ICVs; this point of intersection is called the “venous angle.” The ICVs then course between the roof of the third ventricle and the fornices. Choroid veins, which lie along the floor of the lateral ventricle, also drain into ICVs (Fig. 5.3) [4].

The BVR originates from the intersection of the anterior cerebral vein, DMCV, and striate vein [2,4]. The great cerebral vein (i.e., the vein of Galen, VofG) originates from the intersection of two ICVs and the BVR. VofG is a 2-cm long, U-shaped midline vein that courses under the splenium of the corpus callosum in the quadrigeminal cistern [4]. The VofG and ISS intersect to form straight sinuses [3].

Brain Stem and Posterior Fossa Veins

The brain stem and posterior fossa veins are categorized into three subgroups according to their drainage system [2,3]:

- *Superior (Galenic) Group:* This group includes precentral cerebellar (PCV), superior vermian (SVV), and anterior pontomesencephalic veins (APMV). The PCV courses between the lingual and central lobule

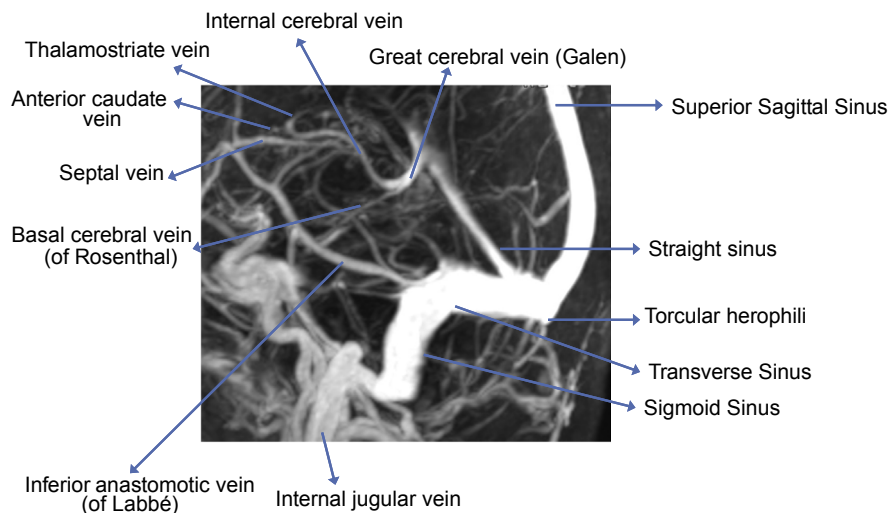


FIGURE 5.2 Cerebral veins of deep circulation and posterior fossa are shown in lateral view MR venography. Dominant structure of this system is great cerebral vein (of Galen), which is formed by joining of two internal cerebral veins, and basal cerebral vein of Rosenthal. Then it drains into straight sinus together with inferior sagittal sinus.

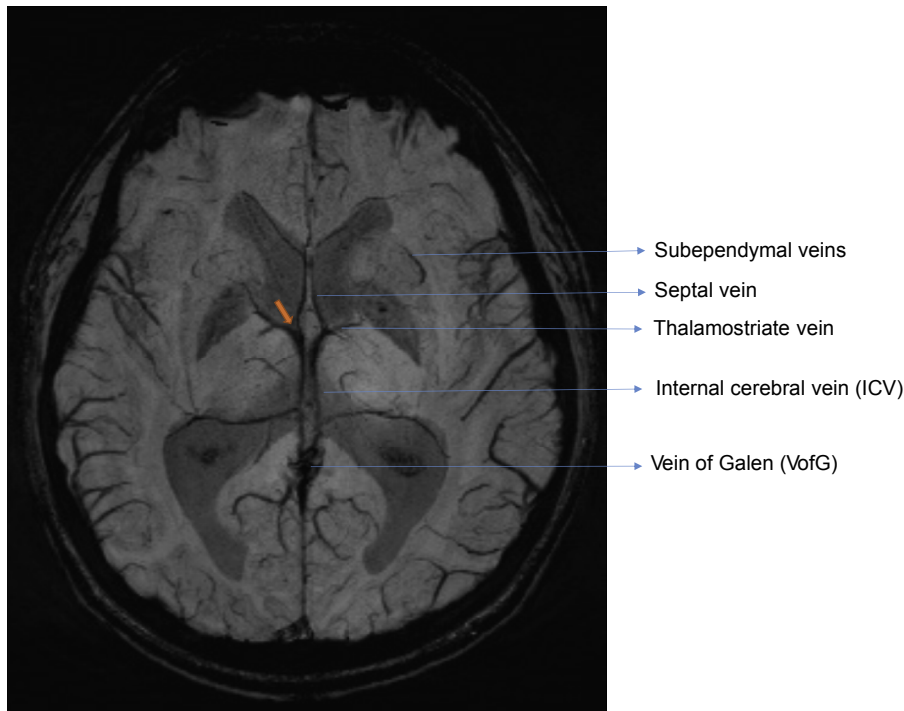


FIGURE 5.3 Axial imaging of susceptibility-weighted (SW) magnetic resonance shows septal vein and thalamostriate vein which meet near the foramen of Monro and are composed of internal cerebral vein. This point of intersection is called the “venous angle” (orange arrow). The great cerebral vein (of Galen) originates from the intersection of two internal cerebral veins and basal vein of Rosenthal.

of vermis. The superior vermian vein originates from the top of the vermis, courses through the culmen, and drains into the PCV. The APMV includes many smaller veins that cover the cerebral peduncles and anterior surface of the pons. All veins in this group drain into the VofG.

- *Anterior (Petrosal) Group:* The petrosal vein (PV) is the dominant vascular structure of this group, which is important during cerebellopontine angle cistern surgery. Tributaries from the brain stem and cerebellum are observed as a “petrosal star” on DSA or computed tomography venography (CTV). The PV forms an anastomosis with the lateral mesencephalic vein and SPS [2].
- *Posterior (Tentorial) Group:* The inferior vermian veins lie under the vermis and receive tributaries from the inferior part of the cerebellum.

References

- [1] Kiliç T, Akakin A. Anatomy of cerebral veins and sinuses. *Front Neurol Neurosci* 2008;23:4–15.
- [2] Osborn AG. Veins and Venous Sinuses. In: Harnsberger HR, Osborn AG, Macdonald AJ, Ross JS, Moore KR, Salzman KL, Wiggins RH, Davidson HC, Hamilton BE, Carrasco CR, editors. Utah: Amirsys Publishing; 2011. p. I 334–87.
- [3] Rhoton Jr AL. The cerebral veins. *Neurosurgery* 2002;51(4 Suppl.):159–205.
- [4] Uddin MA, Haq TU, Rafique MZ. Cerebral venous system anatomy. *J Pak Med Assoc* 2006;56(11):516–9.
- [5] Ayanzen RH, Bird CR, Keller PJ, McCully FJ, Theobald MR, Heiserman JE. Cerebral MR venography: normal anatomy and potential diagnostic pitfalls. *AJNR Am J Neuroradiol* 2000;21(1):74–8.
- [6] Yasuda A, Campero A, Martins C, Rhoton Jr AL, de Oliveira E, Ribas GC. Microsurgical anatomy and approaches to the cavernous sinus. *Neurosurgery* 2008;62(6 Suppl 3):1240–63.
- [7] Tubbs RS, Bosmia AN, Shoja MM, Loukas M, Curé JK, Cohen – Gadol AA. The oblique occipital sinus: a review of anatomy and imaging characteristics. *Surg Radiol Anat* 2011;33(9):747–9.

CHAPTER

6

Cerebral Vasa Vasorum

W.M. Ho¹, C. Reis², O. Akyol¹, J. Zhang^{1,2}

¹Loma Linda University School of Medicine, Loma Linda, CA, United States; ²Loma Linda University Medical Center, Loma Linda, CA, United States

INTRODUCTION

Vasa vasorum (VV) are defined literally as vessels of vessels, and are predominantly observed in large vessels with an important role under pathological conditions. Research on noncerebral VV has been established for over a century, including cardiac, pulmonary, aortic, and portal vein VV. Intracranial vessels were misrepresented to be devoid of VV, and increasing evidence for their existence widens the field of cerebral VV research. Constantly improving technology and modern radiologic methods reveal new aspects of intra- and extracranial cerebral VV, and provide further elucidation on how they act in neurovascular disease. However, cerebral VV remain a highly discussed topic with contradicting and discrepant theories [1].

STRUCTURE, FUNCTION, AND LOCALIZATION

VV are considered microvessels within the wall of a host vessel, forming a microvascular network predominantly in large arteries. Their main functions are supplying oxygen and nutrients to the adventitia and the outer media and eliminating waste, while the inner vascular layers are nourished by intraluminal blood diffusion.

Cerebral arteries compared to systemic vessels have a thinner tunica media and adventitia. Instead of an external elastic lamina, there are only few elastic fibers, and the internal elastic lamina is fenestrated [1]. Further, tiny openings of 1–3 μm diameter were observed on the surface of intracranial vessel walls,

which connects the tunica media with the cerebrospinal fluid (CSF). Zervas et al. described that these small channels enable CSF to get in contact with deeper layers of the vessel walls, building an adventitial network called the rete vasorum [1–3]. These differences compared to systemic vessels enable intracranial arteries to be nurtured by CSF diffusion, therefore decreasing the demand for supplemental nourishment by VV [1,2]. Animal studies in canine, feline, and rodents confirmed the lack of VV in cerebral vessels, the same as in an examination of intracranial arteries of neonates and children without cerebrovascular diseases [2]. This suggests that intracranial VV do not exist at birth [1]. However, small capillary-like vessels of 10–20 μm in diameter were detected in adult patients, consistent with VV [3]. They were predominantly localized in the proximal part of the internal carotid arteries, the basilar, and vertebral arteries [2–4]. Cerebral VV were reported in even further distal arteries in two studies, but not in the distal part of the middle and anterior cerebral artery. The reason for the discrepancy might be including vessels with smaller diameter and different patient selection in rather small cohort studies. Connolly et al. suggested an association of VV with the enlargement of vessel and intima thickness, using highly sensitive and specific immunohistochemical staining of Factor VIII [3]. In a similar study by Aydin et al., no VV were seen in arteries with a tunica media of less than 250 μm thickness, disregarding the size of systemic arteries. Furthermore, cerebral VV were observed for a distance of 1–1.5 cm after dural penetration following the proximal intracranial internal carotid artery and vertebral artery [4]. Regarding the layers in the vessel wall, cerebral VV are localized almost exclusively in the tunica adventitia, but rarely in the media [3,4](Figs. 6.1 and 6.2).

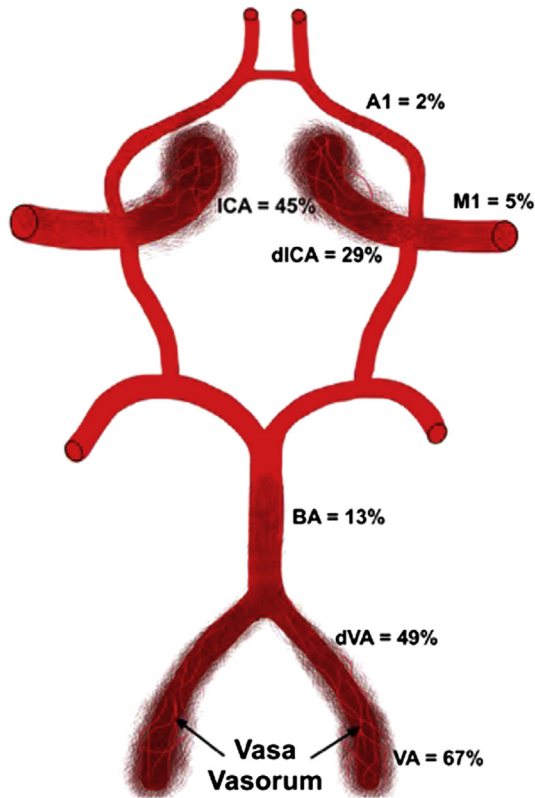


FIGURE 6.1 Localization and incidence of cerebral vasa vasorum (VV). Percentage numbers are derived from the light microscopical investigation by Takaba and colleagues of 50 patients with intracranial diseases, such as aneurysm, intracerebral hemorrhage, stroke, brain tumor, or trauma [4]. Cerebral VV most frequently occurred in the vertebral artery (VA), distal segment of the vertebral artery 1 cm proximal to the formation of the basilar artery (dVA), internal carotid artery (ICA), and distal segment of internal carotid artery to origin of posterior communicating artery (dICA). They are less likely to occur in the basilar artery (BA), proximal M1-part of the middle cerebral artery, and proximal A1-part of the anterior cerebral artery.

CEREBRAL VASA VASORUM NEOVASCULARIZATION

All published data so far agree in terms of a direct correlation between VV incidence and cerebrovascular disease, although whether cerebral VV development is the cause or the response remains poorly understood. Most pathophysiological research on VV neovascularization has been on cardiovascular and pulmonary arteries. However, few experimental investigations on cerebral VV assume similar angiogenic pathways involved in cerebral neovascularization as in other VV [5,6]. There is evidence that VV neovascularization is associated with cardiovascular risk factors and both initiation as well as progression of atherosclerosis. Hypertension and intimal thickening as a response to atherosclerosis leads to insufficient oxygen and nutrient diffusion. Thicker intima and plaque growth becomes a diffusion obstacle for intraluminal nourishment,

thereby contributing to a hypoxic response and vascular cell damage. As a compensatory mechanism to oxygen and nutritional demand, VV neovascularization is induced, and preexisting VV grow deeper toward the vessel lumen to support the supply of the inner layers. Underlying pathophysiological signaling pathways involve hypoxic inducible factor (HIF) as a key regulator of atherosclerosis and angiogenic response, although multiple pathological triggers are assumed to be involved. HIF is known to activate vascular endothelial growth factor (VEGF) and E26 transformation-specific (Ets) factor, both are important enhancers of hypoxia-induced angiogenesis and VV development. VEGF is strongly correlated with neovascularization and angiogenic sprouting under physiological and pathophysiological circumstances. In a hypertensive rat model, elevated expression of VEGF and HIF coincided with VV growth in the aorta. Ets is a transcription factor that regulates gene expression of matrix metalloproteinases (MMPs), and therefore contributes to extracellular matrix degradation and migration of vascular endothelial cells supporting VV neovascularization. Additionally, Ets upregulates the angiogenic factors, hepatocyte growth factor, and VEGF. Besides VEGF and Ets, multiple other mechanisms are involved in VV neovascularization with either synergistic or independent effects on angiogenesis, including fibroblast growth factors (FGF) and epidermal growth factor [7,8].

Interestingly, vascular occlusion seems to be a stronger catalyst than atherosclerosis alone for promoting both intra- and extravascular neovascularization [2]. A major contributor to VV neovascularization is initiation and perpetuation via vascular inflammation caused by intraluminal monocyte adhesion, lipid oxidation, and increased release of cytokines or growth factors. Consequently, neovessels are most likely present where chronic inflammatory cells, such as macrophages and lymphocytes, infiltrate the vessel wall. Novel publications support the hypothesis of vascular inflammation initiated in the tunica adventitia and its advance toward the intima. As mentioned before, lipid oxidation and reactive oxygen species cause vascular inflammation, hence VV formation is suggested to be lipid dependent. For instance, oxidized lipids 15-Deoxy- δ -12 and 14-prostaglandin J2 promote neovascularization by activating PPAR- γ , which upregulates VEGF expression in vascular smooth muscle cells. Furthermore, cholesterol modulates lipid rafts in upregulating VEGF signaling-dependent angiogenesis. Supporting the hypothesis, that lipid-dependent vascular inflammation originates in the adventitia, perivascular adipose tissue is assumed to support angiogenesis, especially in advanced stages of atherosclerosis, when neovessels might emit inflammatory mediators to the vascular network of the adipose tissue [7,8].